AD630065

BRL R 1304

BRL

AD

REPORT NO. 1304

DESIGN, OPERATION AND PRELIMINARY RESULTS OF THE BRL EXPANSION TUBE

by

Joseph H. Spurk

October 1965

Distribution of this document is unlimited.

U. S. ARMY MATERIEL COMMAND
BALLISTIC RESEARCH LABORATORIES
ABERDEEN PROVING GROUND, MARYLAND

BALLISTIC RESEARCH LABORATORIES

REPORT NO. 1304

OCTOBER 1965

DESIGN, OPERATION AND PRELIMINARY RESULTS OF THE BRL EXPANSION TUBE

Joseph H. Spurk

Exterior Ballistics Laboratory

Distribution of this document is unlimited.

RDT&E Project No. 1P222901A201

ABERDEEN PROVING GROUND, MARYLAND

B A L L I S T I C   R E S E A R C H   L A B O R A T O R I E S

REPORT NO. 1304

JHSpurk/blw
Aberdeen Proving Ground, Md.
October 1965

ESIGN, OPERATION AND PRELIMINARY RESULTS OF THE BRL EXPANSION TUBE

ABSTRACT

This paper describes the Ballistic Research Laboratories (BRL) expansion tube, which has been built for interferometric observation of hypersonic flow fields. The optical instrumentation consists of a Mach-Zehnder interferometer in conjunction with a rotating mirror and frame camera. By means of simultaneous streak interferometry the free stream conditions are monitored and determined for each test run. With the free stream condition known, the frame interferogram of the flow around the model can be evaluated to give density or electron density field around the model. Examples of density distribution in the free stream are shown for two typical cases, with flow velocity of ~ 10,000 and 20,000 ft/sec, respectively. The density distribution within the shock layer of a reacting flow is shown and compared with theoretical prediction. Conical flow tests are performed in an attempt to asses the free stream turbulence. The effects of second diaphragm and the flow contamination are discussed.

TABLE OF CONTENTS

LIST OF FIGURES

1. INTRODUCTION

The high enthalpy level encountered near the body of a vehicle traveling at hypersonic velocity can be conveniently simulated using a conventional shock tube; however, the Mach number of the supersonic flow behind the shock wave is low and limited.

Since duplication of free stream Mach number is important for many flow conditions of interest, the shock tube has been modified to generate high enthalpy hypersonic flows. In the modification most widely used, a divergent nozzle is attached to the end of the shock tube,[1*] so that the gas behind the shock can be expanded to higher Mach numbers. The main difficulties associated with these types of "shock tunnels" are the extreme reservoir conditions necessary to duplicate ambient flow, and the nonequilibrium state of the test gas.

In order to circumvent these difficulties, an unsteady constant area expansion has been proposed for expanding the gas behind the shock. For the same reservoir condition, an unsteady expansion is more "efficient" in producing high velocities for a small portion of the test gas. The highest obtainable velocity for an unsteady expansion of a perfect gas is

$$u_m = \frac{2}{\gamma-1} a_o$$

while it is only

$$u_m = \sqrt{\frac{2}{\gamma-1}}\ a_o$$

for a steady expansion.

A theoretical feasibility study of this modified shock tube, termed expansion tube, has been reported.[2] Although the expansion tube has theoretically the potential of duplicating a large range of ambient flow conditions, several practical problems arise, typical for an expansion tube. Besides the very short testing times inherent to a facility using unsteady expansion, difficulties arise which are associated with the secondary diaphragm rupture, which can produce disturbances and high turbulence level in the test gas as well as excessive interface mixing.

---

* *Superscript numbers refer to references which may be found on page 40.*

This report describes the design characteristics of the Ballistic Research Laboratories expansion tube and the instrumentation technique used to determine the state of the test gas and to assess the steadiness and duration of the usable flow portion; representative results are given.

The expansion tube has been developed as part of our experimental and analytical research program on hypersonic reacting flows.

2. DESIGN CHARACTERISTICS

Although the expansion tube is primarily intended for the high Mach number and enthalpy range not accessible by shock tunnels, it is quite attractive in the performance range of the latter, due to its lower cost and flexibility; it is also operable as a shock tube.

The BRL expansion tube has been designed as pilot model for interferometric studies of hypersonic nonequilibrium flows in a 10,000 to 20,000 ft/sec velocity range. Interferometry is especially well adapted to short duration events, since testing time is not a major problem.

The design makes use of surplus gun barrels for the major components, driver, driven and expansion sections; it is illustrated in Figure 1. It is noted that the driver and driven section are comparatively short, and enclosed by another tube connecting the three sections. The diaphragm support between driver and driven section incorporates an area reduction. The larger diameter of the driver section just about compensates for the derogatory effect of the area reduction on the shock strength.

A test section with square cross-section of 6.426 inches is fitted to the expansion section, to allow two-dimensional outer flow at the test station, which is necessary for interferometric observation. The transition from round to square cross-section is accomplished by a transition piece, without changing the cross-sectional area. Observation windows are installed in the sidewalls of the test section. The transition piece is described in the Appendix. A "dump tank" is provided to prevent strong reflections and to keep the final discharge pressure below a limit imposed by the strength of the windows. Since the expansion section is very stiff (175mm gun barrel), the facility can be supported by essentially two supports designed to take up the recoil of the tube assembly through elastic deformation.

The pumping system consists of a high pressure Corblin compressor for pressurizing the driver, and a Kinney pump in connection with a 16-inch diffusion pump to evacuate the driven and expansion section, respectively.

3. INSTRUMENTATION

The determination of the state of the test gas poses a serious problem in hypersonic facilities such as arc tunnels, shock tunnels and expansion tubes. The instrumentation adopted for the expansion tube allows a simultaneous investigation of free stream flow and the flow around a model. This technique is, in principle, applicable to other hypersonic facilities as well.

A Mach-Zehnder interferometer is used in conjunction with rotating mirror and frame camera.[3] By means of streak interferometry the free stream flow just ahead of the model is observed in green monochromatic light; the duration of the light source is adjustable from 200 to 600 μsec. The streak interferogram records the varying flow conditions from the arrival of the secondary shock to the arrival of the contact front and expansion fan at the test station (Fig. 2). The streak interferogram is obtained by observing the flow through slits, and sweeping the image on a film drum. The slits are adjusted normal to the axis of the tube, without obstructing the field of view used for the frame interferogram.

An example of a streak interferogram is Figure 3. The fringe shift as displayed in Figure 3 can be reduced to density. Figures 5 and 6 give the density distribution determined from the streak interferogram of Figure 3. The streak interferogram monitors the quality of the free stream flow for each test run. At a preset time after arrival of the shock at the test station, a frame interferogram of the flow around the model is taken in blue monochromatic light of 1-2 μsec duration. The time of the frame picture is indexed on the streak interferogram.

Figure 4 shows a schematic of the optical arrangement. With the density and the static pressure known, the static temperature can be determined for a test gas in chemical equilibrium. For the flow condition reported here, the assumption of chemical equilibrium in the test section can be made, since the unsteady expansion proceeds from a practically undissociated state. (The compressibility in region 2 is less than 1.01).

The optical system can be converted to a streak-schlieren system with observation slit parallel to the tube axis.

Shock-mounted pressure gages in the sidewall of the test section and expansion chamber record the static pressure and measure the shock speed (accuracy +2 to -4 percent).

4. OPERATION

The facility is operated with free stream conditions giving appreciable nonequilibrium flow over the models. Depending on the gas, this requires flow velocities of about $\sim$ 10,000 ft/sec or 20,000 ft/sec at free stream density of approximately 2 x 10^{-5} [gr/cm^3]. For the velocity range of 10,000 ft/sec, cold helium has been used as driver gas, with pressures p_4 up to 10,000 psia. For the flow range of $\sim$ 20,000 ft/sec, combustion heated helium has been used with 700 psia initial pressure p_4. Ignition of the combustible mixture is accomplished by four exploding wires arranged symmetrically around the axis of the driver. It has been found that the driver length could be reduced to 9-inch length without affecting the flow conditions. Annealed copper diaphragms, without scribing, are used between driver and driven section. Mylar diaphragms of 0.5 to 1.5 x 10^{-3}-inch thickness are used between driver and expansion section for driven pressures p_1 between 2 and 10 psia. The initial pressures in the expansion section ranged between 70 and 200 μ Hg, with air, and 200 to 500 μ Hg with helium as accelerating gas. For a typical run only the static pressure in the driven and expansion section is measured. The long duration light source is triggered upon arrival of the shock at the test section; this trigger signal starts the sweep of the recording oscilloscopes for static pressure, heat transfer, and rotational frequency of the rotating mirror. A delayed signal triggers the framing light source. A marker signal from the light source discharge is displayed with the static pressure to correlate streak and frame interferogram with pressure record.

5. PERFORMANCE

The study reported here was not undertaken to study the performance of an expansion tube with respect to theoretical predictions for inviscid fluid. The theoretical predictions were mostly done for perfect gas, and used only as a guide. Good agreement has been found for shock velocities, while free stream densities were about 50 percent lower than the predicted value. In view of the anticipated problems of flow irregularities and interface mixing, the effort was directed to determine if a portion of the hypersonic flow is sufficiently steady to perform a meaningful experiment.

As mentioned before, the free stream conditions are monitored for each experiment. It is felt that the repeatability of the flow conditions for the same initial condition is too poor to rely on a calibration. The testing time required for interferometric studies can be small (of the order of the time necessary for a fluid particle to travel across the interesting portion of the body), with 10-20 μsec being sufficient. However, it is rather difficult to select the proper delay time. Usually several runs are necessary under the same initial conditions to determine the correct delay time.

Fig. 5 shows the density distribution across the field of view in the free stream flow for different times, Δt, after the ignition of the long duration light source (approximately the time of shock arrival at the test station). The shock speed was measured as u_s = 3500 m/sec. The initial conditions were p_4 = 3700 psia He, p_1 = 7 psia O_2, p_{10} = 200 μ Hg air. Provisional windows are used so that only ~ 2.8 inches of the total 6.42-inch test section height are viewed. This is raw, unsmoothed data; the scatter gives an indication of the accuracy of the measurement. Fig. 6 shows the density history for three traces near the centerline. The static pressure trace is plotted also on Fig. 6. Note that the contact surface can be detected in the static pressure trace. Fairly constant pressure and density distributions prevail for about 60 μsec. The density distribution for Δt = 228 μsec and Δt = 280 μsec in Fig. 5 with a minimum in the centerline is characteristic for the distributions measured during the testing time and is thought to be caused at least partly by the recessed (1/8-inch) provisional windows. The trace for Δt = 342 μsec is taken in the expansion fan. Fig. 7a is the actual pressure record of Figure 6. Figure 7b shows a typical pressure record for shock velocities of ~ 6500 m/sec.

Figs. 8 and 9 show the density distribution across the field of view for a test run at shock velocity u_s = 6460 m/sec with dry air as test medium. The initial conditions were p_4 = 700 psia He, H_2, O_2 before combustion; p_1 = 8 psia dry air; p_{10} = 70 μ Hg air. Note the similarity of the density profile at 120 μsec with the profiles of Fig. 5. The distribution at Δt = 155, 185 and 230 μsec are taken in the expansion fan. In Fig. 10 the corresponding density history for three traces is plotted together with the static pressure trace (original not suitable for reproduction). Here too the contact surface can be detected in the static pressure signal. The time for which pressure and density is fairly constant is about 40 μsec. The resolution of this streak interferogram is approximately 2 μsec. The time resolution depends on the rotational speed of the rotating mirror and on the duration and intensity of the backlight. The system is capable of 0.2 μsec resolution.

The density values obtained from interferometry are average values across the width of the test section. Locally, the fluctuation of the density may well be larger than indicated by Figures 5 through 9. In order to assess local irregularities in the flow field, conical flow tests have been performed. It can be shown[4] that for conical flow field plots of the quantity δ/x versus r/x must collapse into a single curve. δ is the fringe shift at a point r,x in a cartesian coordinate system at the vertex of the cone. The conical flow test is approximately valid for reacting flow around a cone. Figure 11 shows the result of a conical flow test for the flow of Fig. 16. For comparison, Figure 11 includes a conical flow test[4] for a cone fired in a ballistic range under very low free stream turbulence. The scatter of the data is seen to be about the same in both cases. It may be concluded that no flow disturbances with wavelength in the order of model diameter (1-1/2 inches) exist.

A qualitative estimate of the free stream disturbance can also be obtained by observing the variation of shock standoff distance for a flow over blunt body, as in Figure 12. The standoff distance of a detached shock ahead of a sphere of $1\frac{1}{4}$-inch diameter is viewed through a slit parallel to the tube axis by means of streak schlieren. Only a portion of the total record is shown. The shock around the model is established 100 μsec after arrival of the secondary shock at the test station; this is the anticipated beginning of the usable flow regime for a shock velocity of $u_s \sim 6500$ μsec. Figure 13 shows a plot of the standoff distance. The standoff distance is almost constant for about 40 μsec. Similar experiments using a flat-faced cylinder show considerably larger variation of standoff distance up to 20 percent. It is possible that this variation is model induced.

Most of the flow irregularities in an expansion tube have to be attributed to secondary diaphragm effects. The experimental indication is that the secondary diaphragm bursts in rather small pieces. As the test gas passes these pieces it loses momentum and energy in accelerating them and transferring heat to them. For an uneven suspension of these particles, which is the rule, the gas flow will be correspondingly disturbed. It may be noted that an estimate for the effect of the particles on the flow can be made under the assumption of homogenously suspended particles. The particles may then be considered as molecules of a heavy gas, and the problem treated as an unsteady two-phase flow.

Flow contamination by diaphragm particles is another problem associated with the secondary diaphragm. The arrival of the diaphragm particles at the test station may be estimated easily by neglecting the effect of the particles on the outer flow. Assuming that the only force acting on the particles is the drag, the motion is described by

$$\ddot{x} = \frac{\rho}{2}(u-\dot{x})^2 \frac{C_D}{h\,\rho_d} \tag{1}$$

ρ_d being the density of diaphragm material, h the thickness, and C_D the drag coefficient. Note that the acceleration is independent of the size of the particle for particle orientation normal to the flow direction.

With the conditions that for $t = 0$, $\dot{x} = 0$, $x = 0$ ($x = 0$, location of diaphragm) the particle finds itself in the region of constant u and ρ behind the expansion fan for a time $0 < t < t_1$. Then Equation (1) can be integrated

$$x = u_2 t - \frac{\rho_d 2h}{\rho_2 C_D} \ln\left(\frac{\rho_2 C_D}{\rho_d 2h} u_2 t + 1\right) . \tag{2}$$

At time $t = t_1$ the particle enters the expansion fan. For a centered expansion fan u is given by

$$u = \frac{2}{\gamma+1}\frac{x}{t} + \frac{\gamma-1}{\gamma+1}\left(u_2 + \frac{2}{\gamma-1} a_2\right) \tag{3}$$

and

$$\rho = \rho_2 \left[\frac{1}{a_2}\frac{\gamma-1}{\gamma+1}\left(u_2 + \frac{2}{\gamma-1} a_2 - \frac{x}{t}\right)\right]^{\frac{2}{\gamma-1}} \tag{4}$$

With (3) and (4) Equation (1) can be integrated numerically. Fig. 14 shows the particle path for typical initial conditions, assuming various values for C_D. Air has been assumed as an ideal gas for this calculation. In an experimental investigation the first particle visible in streak schlieren was observed 300 μsec after arrival of secondary shock at the test section. (See Table I). If pressure gradients can cause considerable accelerations, particles may arrive earlier at the test station than indicated by the above estimate. Radiation from diaphragm material has indeed been observed during the testing time.[5]

6. RESULTS

Figures 15 through 20 represent frame interferograms of hypersonic flow fields obtained in the expansion tube. Figure 15 shows the flow around a sphere of 1-1/4" diameter in oxygen. The free stream density has been determined to be $\rho = 2.0 \times 10^{-5}$[g/cm^3] and pressure $p = 0.236$ [Dyn/cm^2]; the static temperature is then $T_\infty = 430°$K. The free stream velocity is $u_\infty = 3700$ m/sec, with a corresponding Mach number of 8.9.

Figure 16 shows the flow around a cone-cylinder in oxygen under similar free stream conditions as the flow of Figure 15.

Figures 17 and 18 show two simultaneous frame interferograms of an air flow around a sphere in an attempt to measure the electron concentration. The free stream velocity is $u_\infty \approx 6100$ m/sec. No streak interferogram has been obtained for this run, so that the free stream density cannot be determined. Figure 17 is obtained in blue monochromatic light, and Figure 18 in green monochromatic light. Self-luminosity, as in Figure 18, poses a serious problem in interferometry of high enthalpy flows.

Figure 19 is an interferogram of a hypersonic air flow around a cone-cylinder. The free stream conditions (see Figs. 9 and 10) have been determined to be $\rho_\infty = 1.5 \times 10^{-5}$[g/cm^3], $T_\infty = 719°$K, $p_\infty = 0.31$[Dyn/cm^2], $u_\infty =$ 6460 m/sec, $M_\infty = 12.0$.

The free stream velocities are assumed to be equal to the shock velocities.[6]

The density and derived quantities given above have not been corrected for boundary layer effects on the wall of the test section. The correction can be determined experimentally, though this is not possible with the windows used at present.

Figure 20 is an interferogram in an oxygen flow from which the density distribution within the shock layer has been reduced. In Fig. 21 the experimental density distribution of a trace x = 11.85mm from the tip of the model is compared with theoretical predictions.[3,7] For the theoretical calculation the density as determined from the streak has been increased 10 percent to account for the boundary layer effect. An estimate of the boundary layer effect, assuming ideal gas and flat plate, gives an increase of 17 percent. The overshoot in density near the shock in Fig. 18 is due to the reduction procedure.

JOSEPH H. SPURK

TABLE I

Initial Condition		P_4 psia	P_1 psia	P_{10} mm Hg	U_s km/sec	t_{part} μsec	U_{part} km/sec	U_{part}/U_s
He/Air/Air	(1)	3600	8	.11	3.45	775	2.90	.84
	(2)	3600	8	.07	3.75	1100	2.88	.77
He,H_2,O_2/Air/Air	(1)	700*	8	.16	6.74	300**	6.00	.89
	(2)	700*	8	.06	6.82	540	5.52	.81
	(3)	700*	8	.10	6.50	720	5.28	.81

*Before combustion

**Earliest particle observed

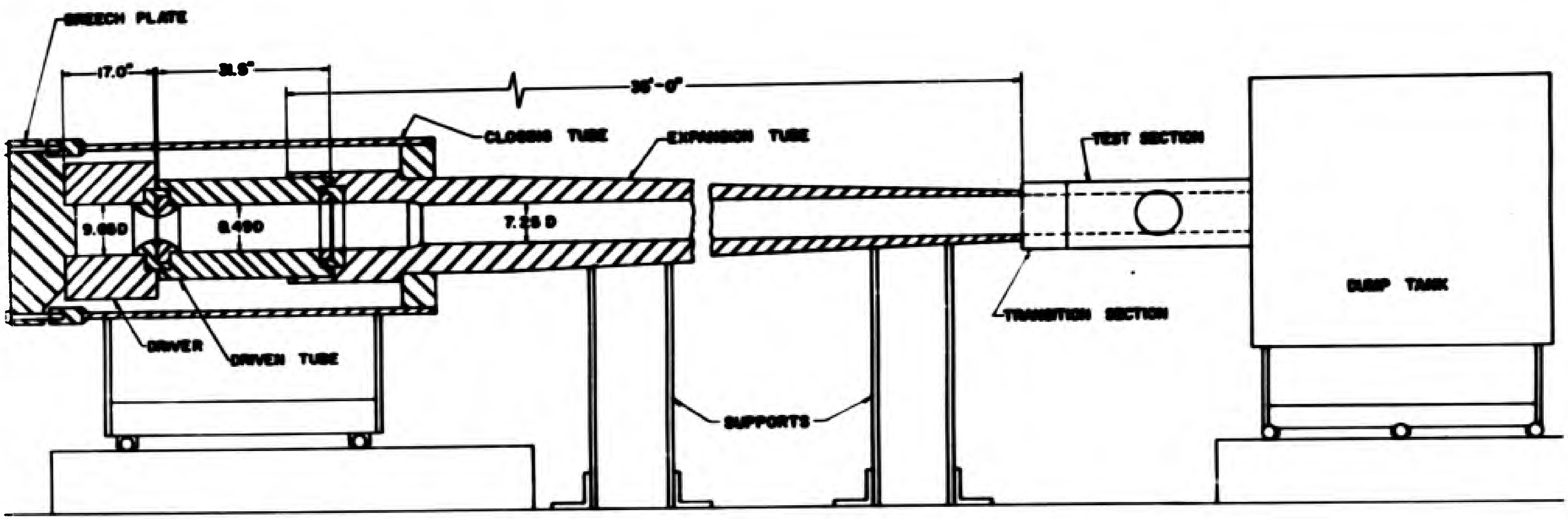
BREECH PLATE
17.0"
31.6"
36'-0"
CLOSING TUBE
EXPANSION TUBE
TEST SECTION
9.060 D
8.490
7.25 D
DUMP TANK
TRANSITION SECTION
DRIVER
DRIVEN TUBE
SUPPORTS

FIGURE 1

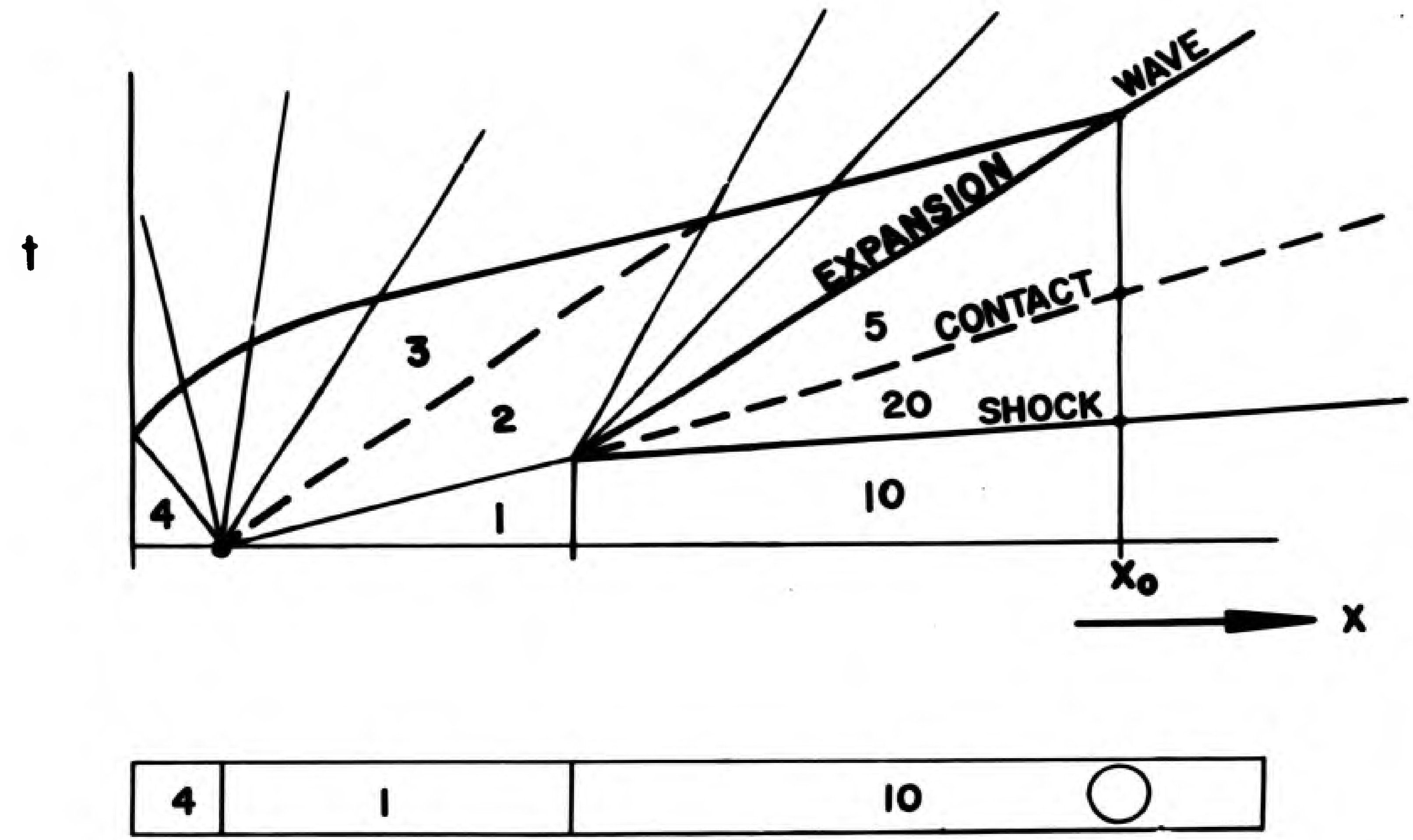

FIGURE 2

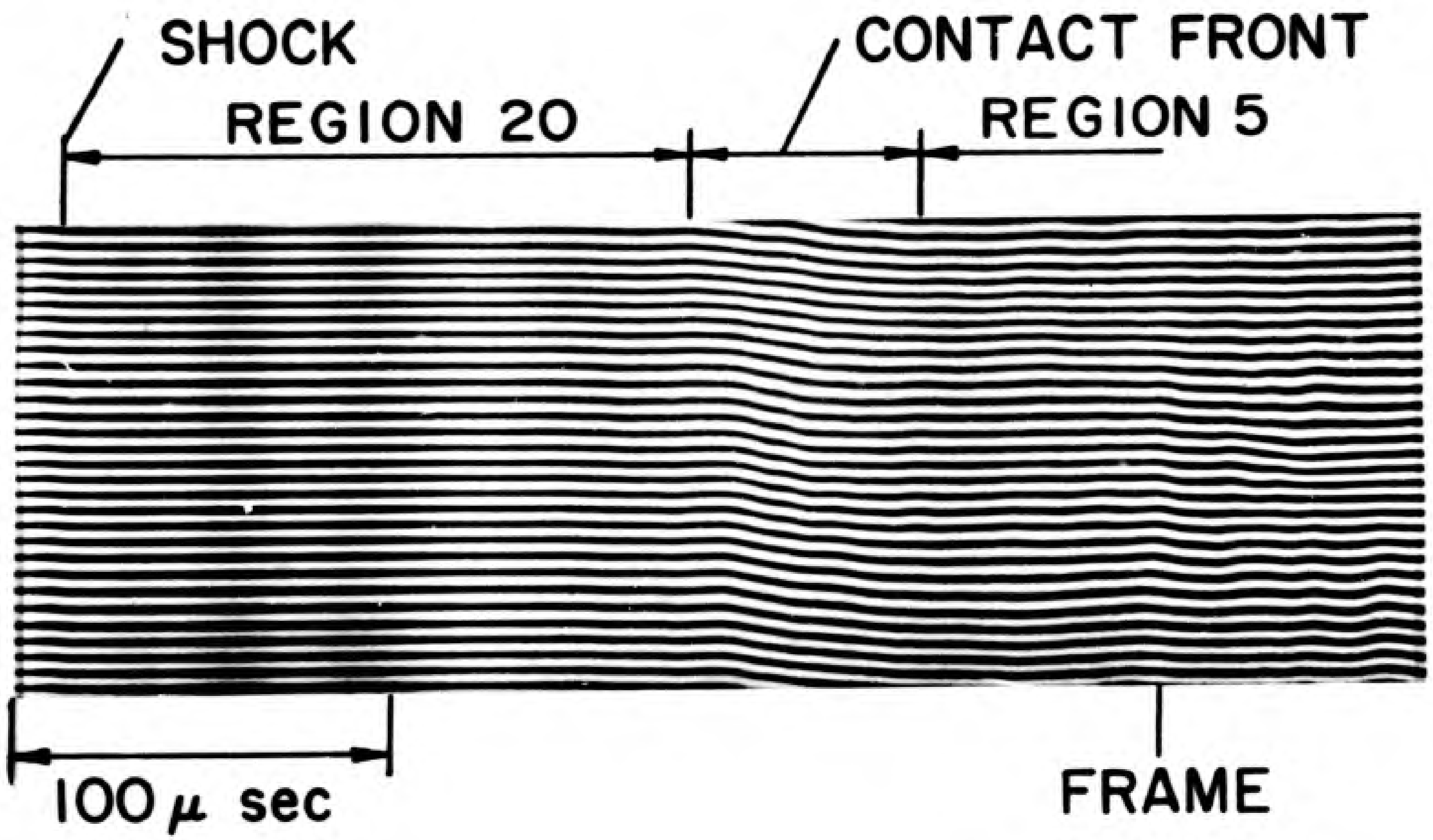

FIGURE 3

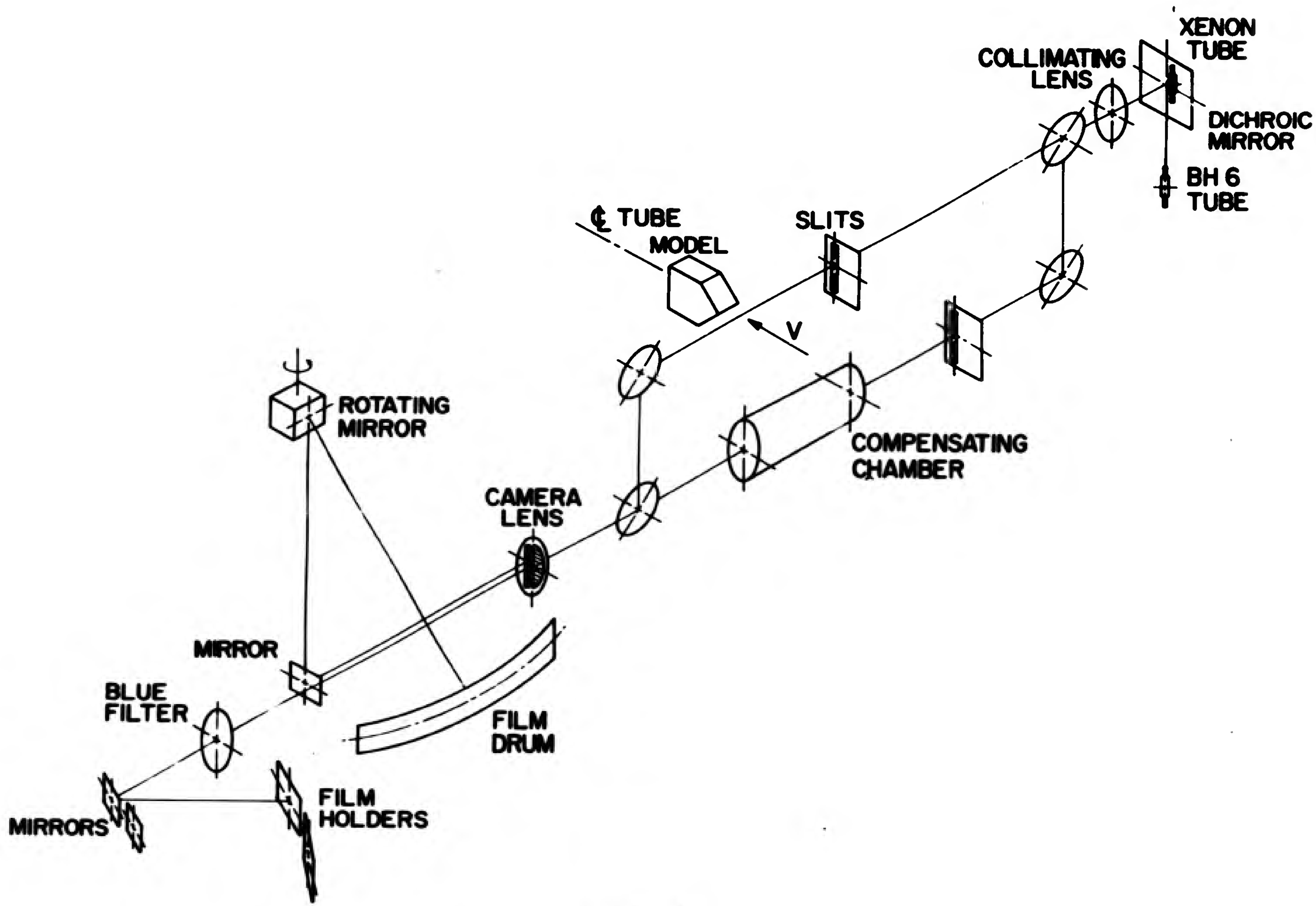
XENON TUBE
COLLIMATING LENS
DICHROIC MIRROR
BH 6 TUBE
℄ TUBE
MODEL
SLITS
V
ROTATING MIRROR
COMPENSATING CHAMBER
CAMERA LENS
MIRROR
BLUE FILTER
FILM DRUM
FILM HOLDERS
MIRRORS

FIGURE 4

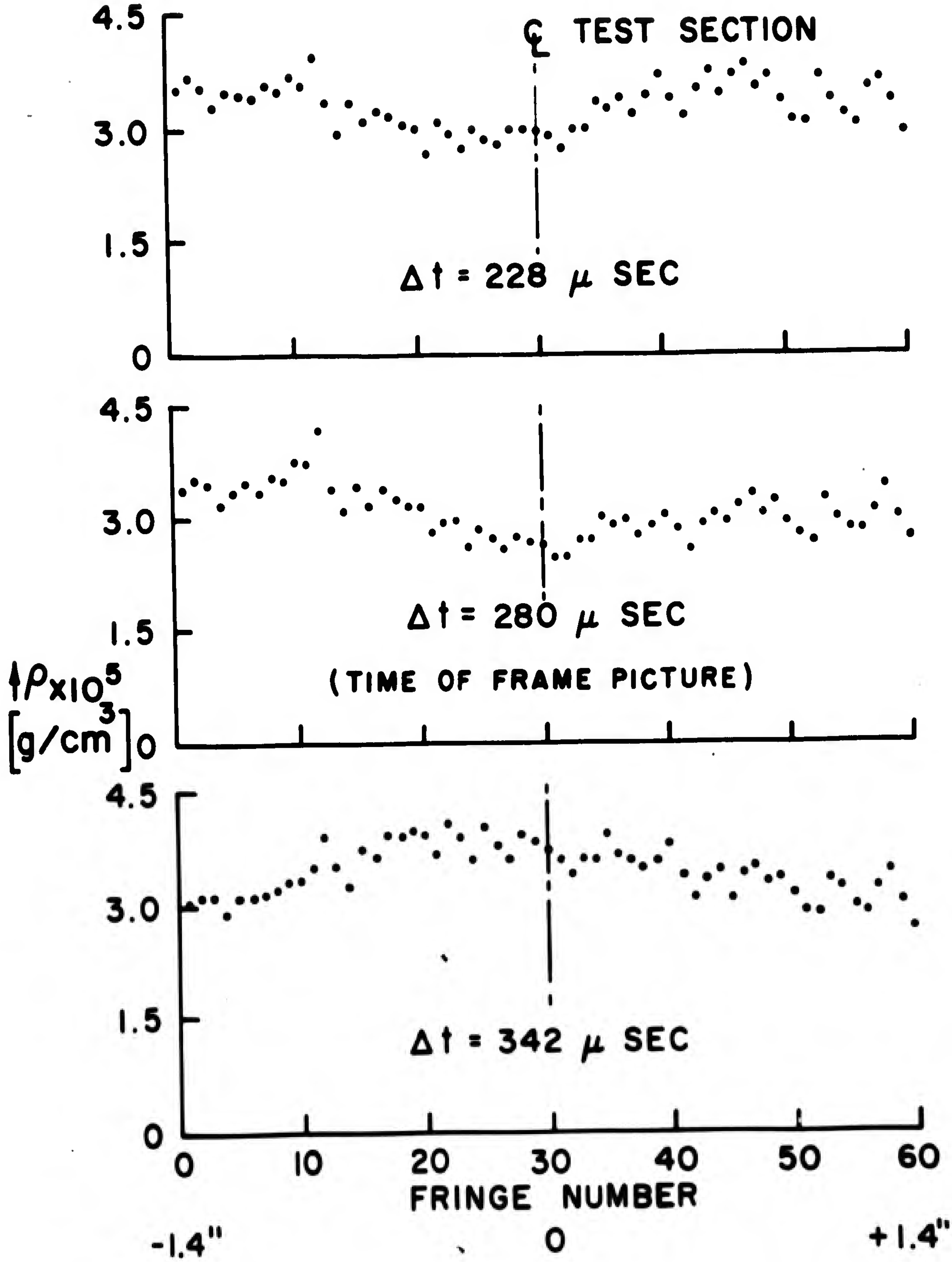

4.5
3.0
1.5
0
℄ TEST SECTION
Δt = 228 μ SEC
4.5
3.0
1.5
Δt = 280 μ SEC
(TIME OF FRAME PICTURE)
↑ρ x 10^5
[g/cm^3]
0
4.5
3.0
1.5
Δt = 342 μ SEC
0
0
10
20
30
40
50
60
FRINGE NUMBER
-1.4"
0
+1.4"

FIGURE 5

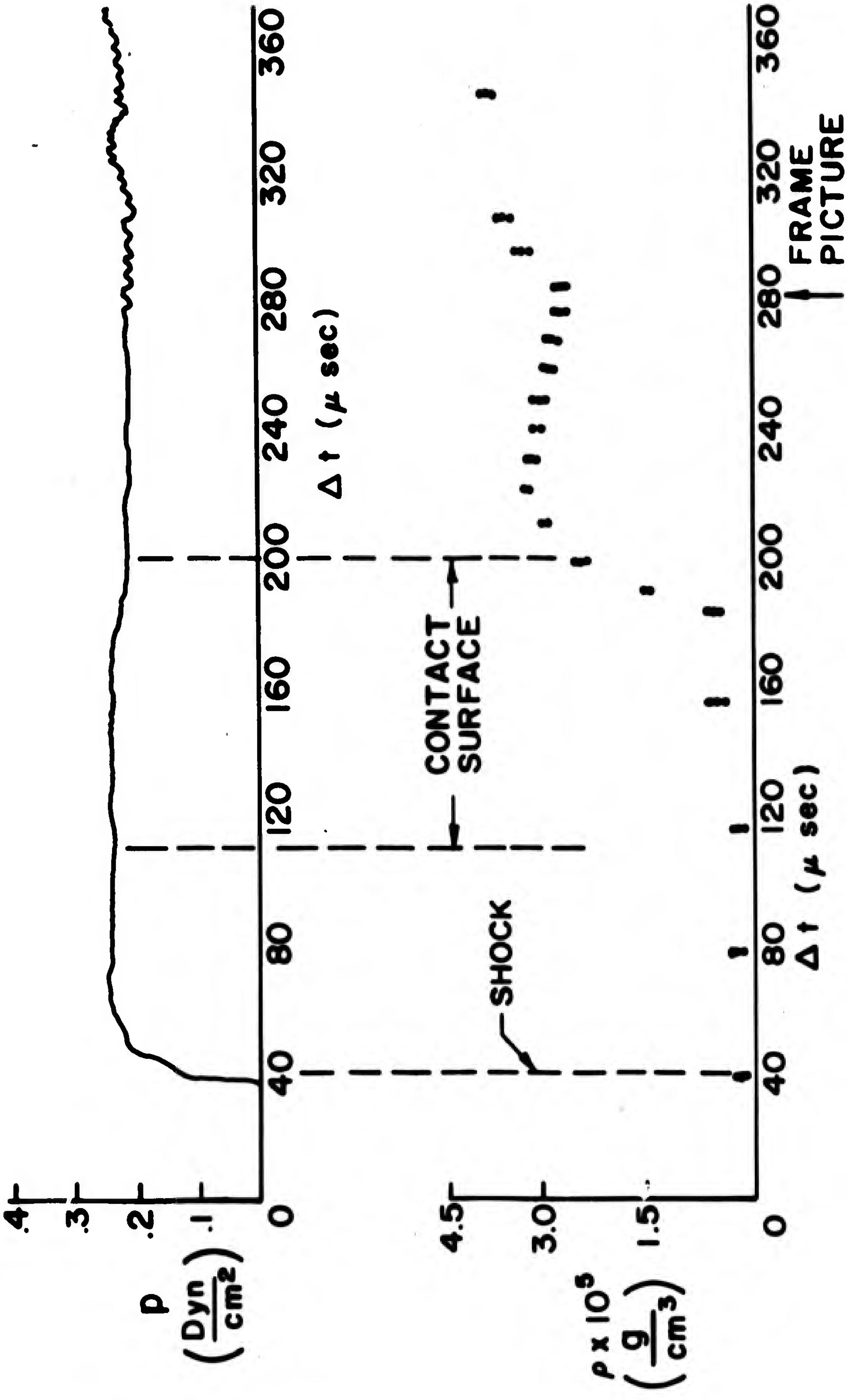

p
(Dyn/cm²)
.4
.3
.2
.1
0
40
80
120
160
200
240
280
320
360
Δ t (μ sec)
SHOCK
CONTACT SURFACE
ρ x 10⁵
(g/cm³)
4.5
3.0
1.5
0
Δ t (μ sec)
FRAME PICTURE

FIGURE 6

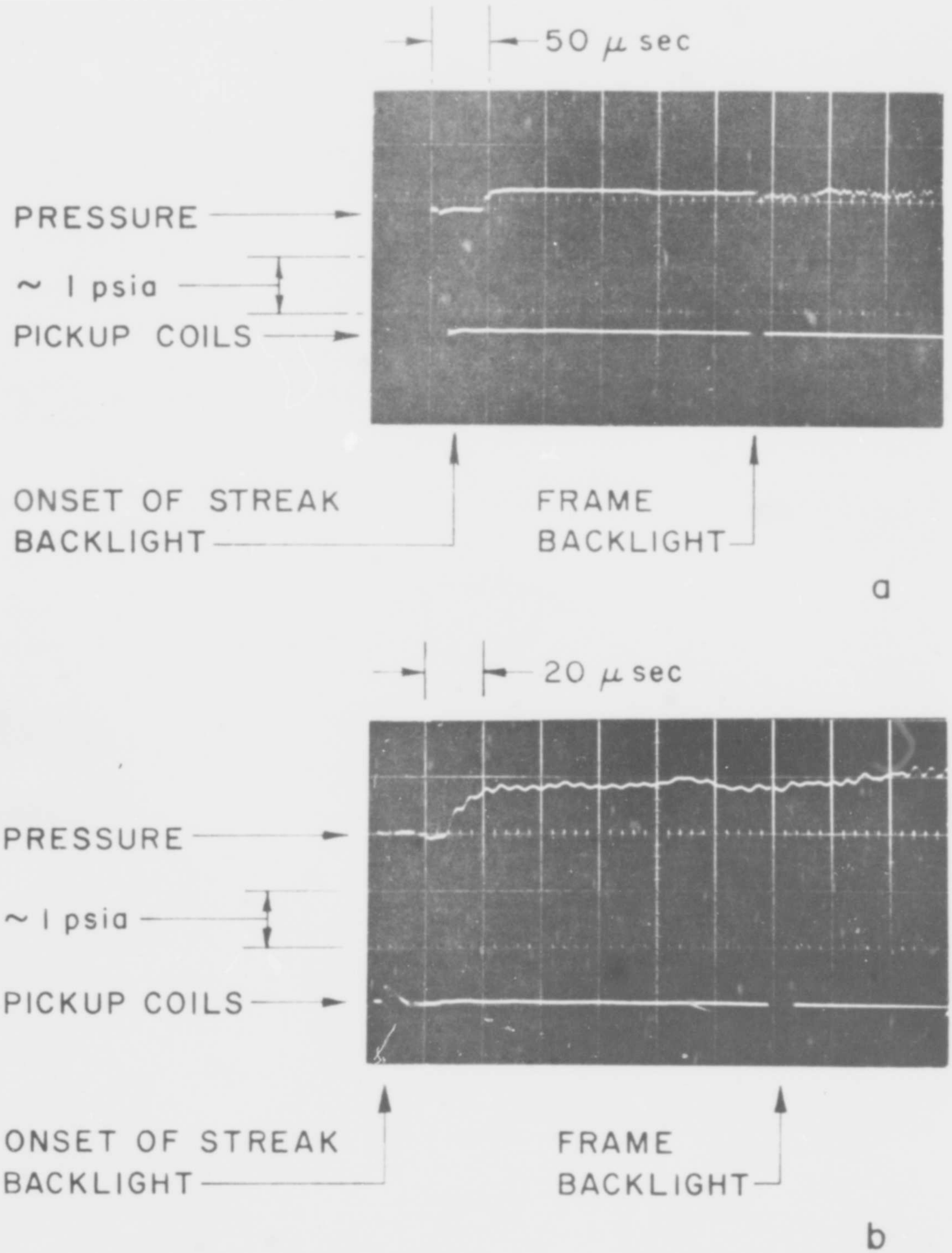

50 μ sec
PRESSURE
~ l psia
PICKUP COILS
ONSET OF STREAK BACKLIGHT
FRAME BACKLIGHT
a
20 μ sec
PRESSURE
~ l psia
PICKUP COILS
ONSET OF STREAK BACKLIGHT
FRAME BACKLIGHT
b

FIGURE 7

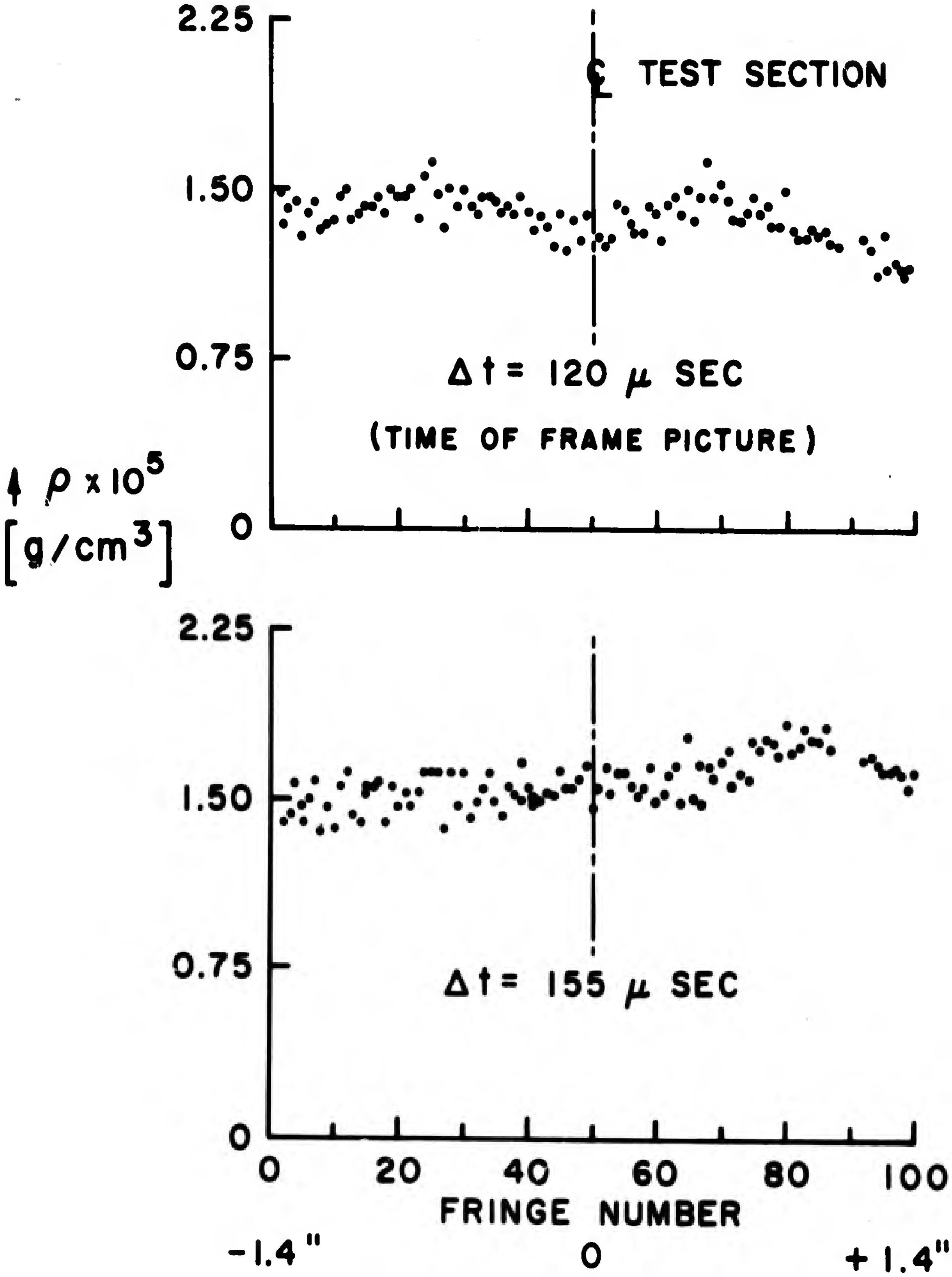

2.25
1.50
0.75
0
℄ TEST SECTION
Δt = 120 μ SEC
(TIME OF FRAME PICTURE)
ρ x 10^5
[g/cm^3]
2.25
1.50
0.75
0
Δt = 155 μ SEC
0
20
40
60
80
100
FRINGE NUMBER
-1.4"
0
+1.4"

FIGURE 8

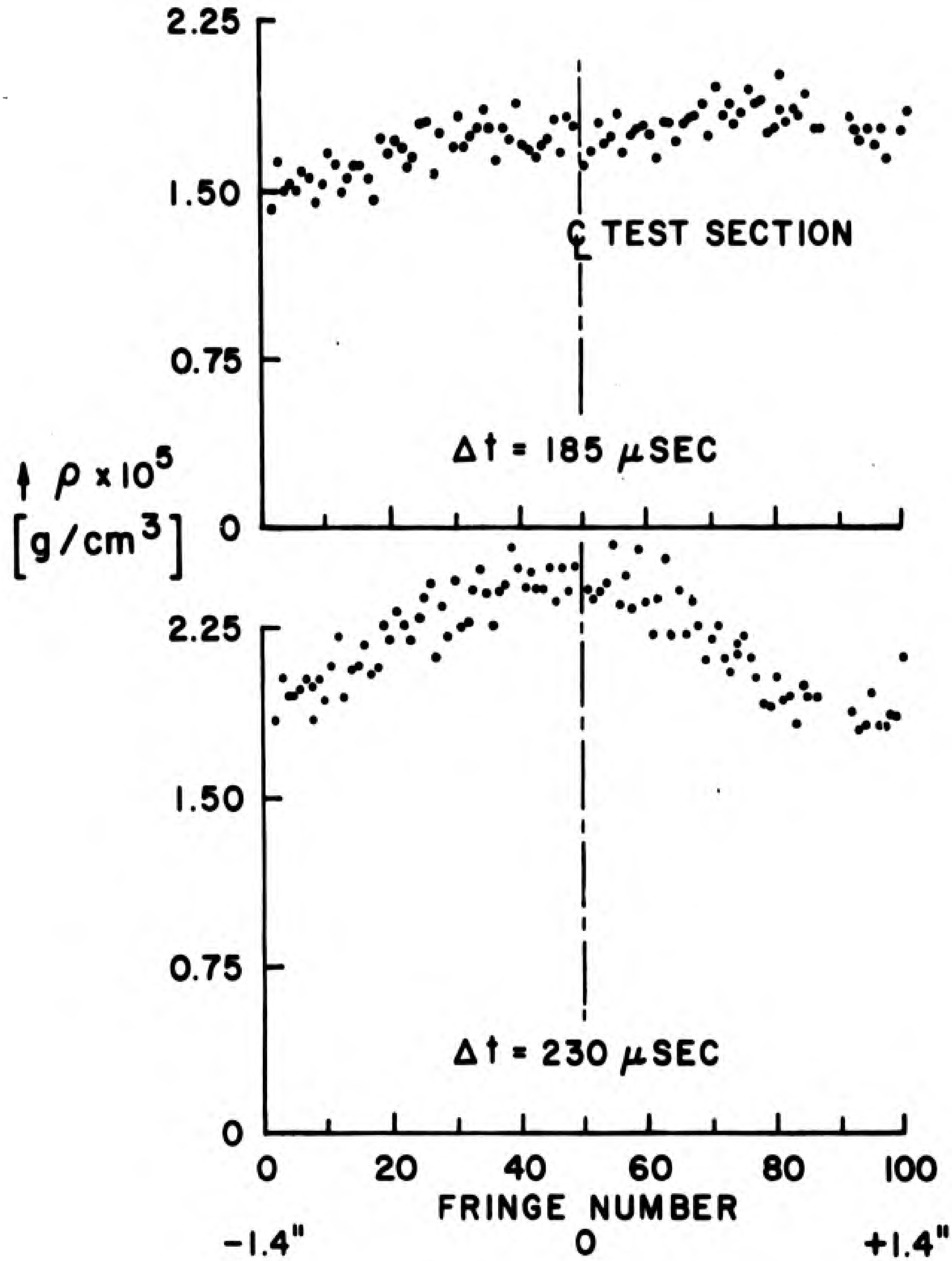
2.25
1.50
0.75
0
℄ TEST SECTION
Δt = 185 μSEC
ρ x 10^5
[g/cm^3]
2.25
1.50
0.75
0
Δt = 230 μSEC
0
20
40
60
80
100
FRINGE NUMBER
-1.4"
0
+1.4"

FIGURE 9

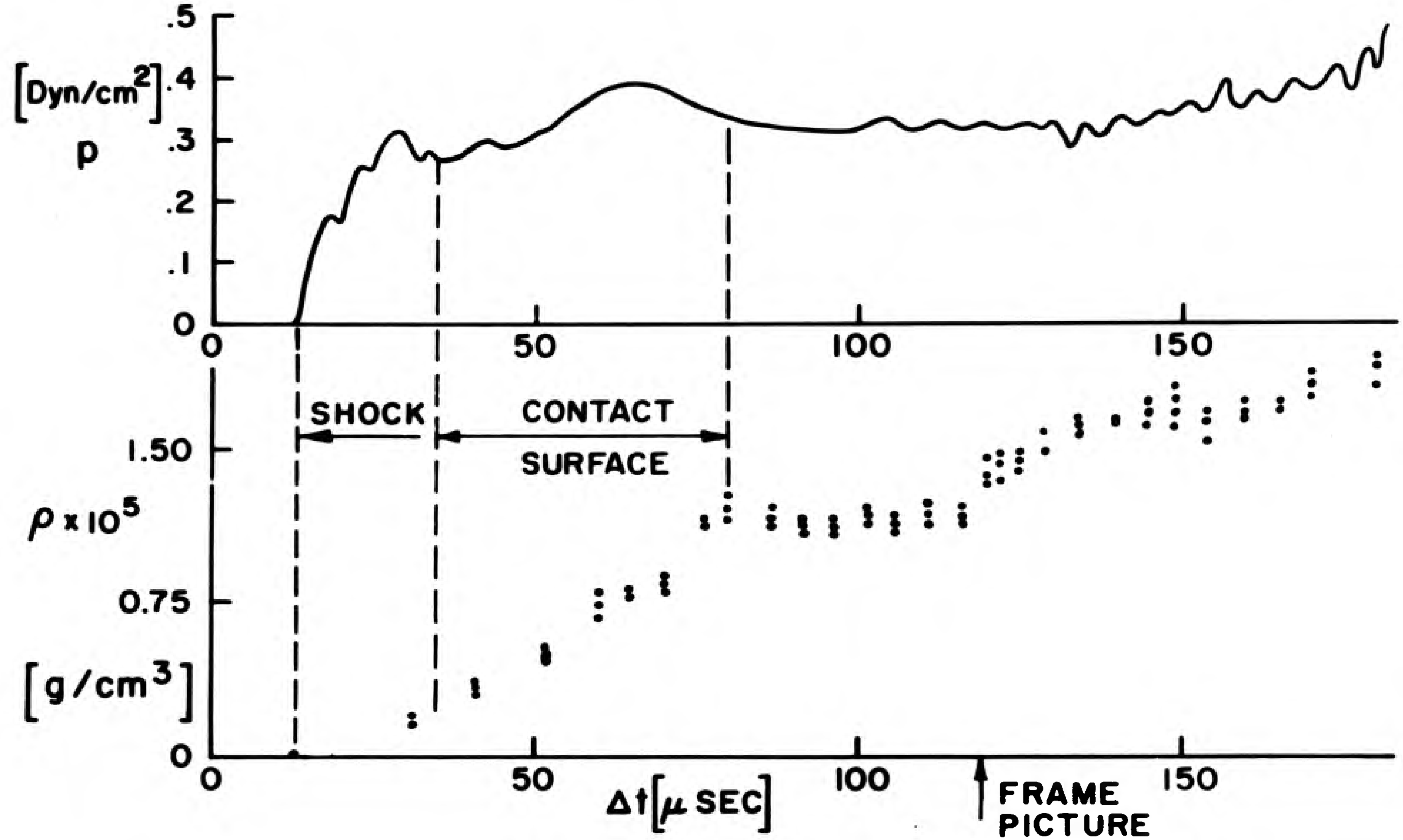
[Dyn/cm²]
p
.5
.4
.3
.2
.1
0
0
50
100
150
SHOCK
CONTACT
SURFACE
1.50
ρ x 10⁵
0.75
[g/cm³]
0
0
50
100
150
Δt[μ SEC]
FRAME
PICTURE

FIGURE 10

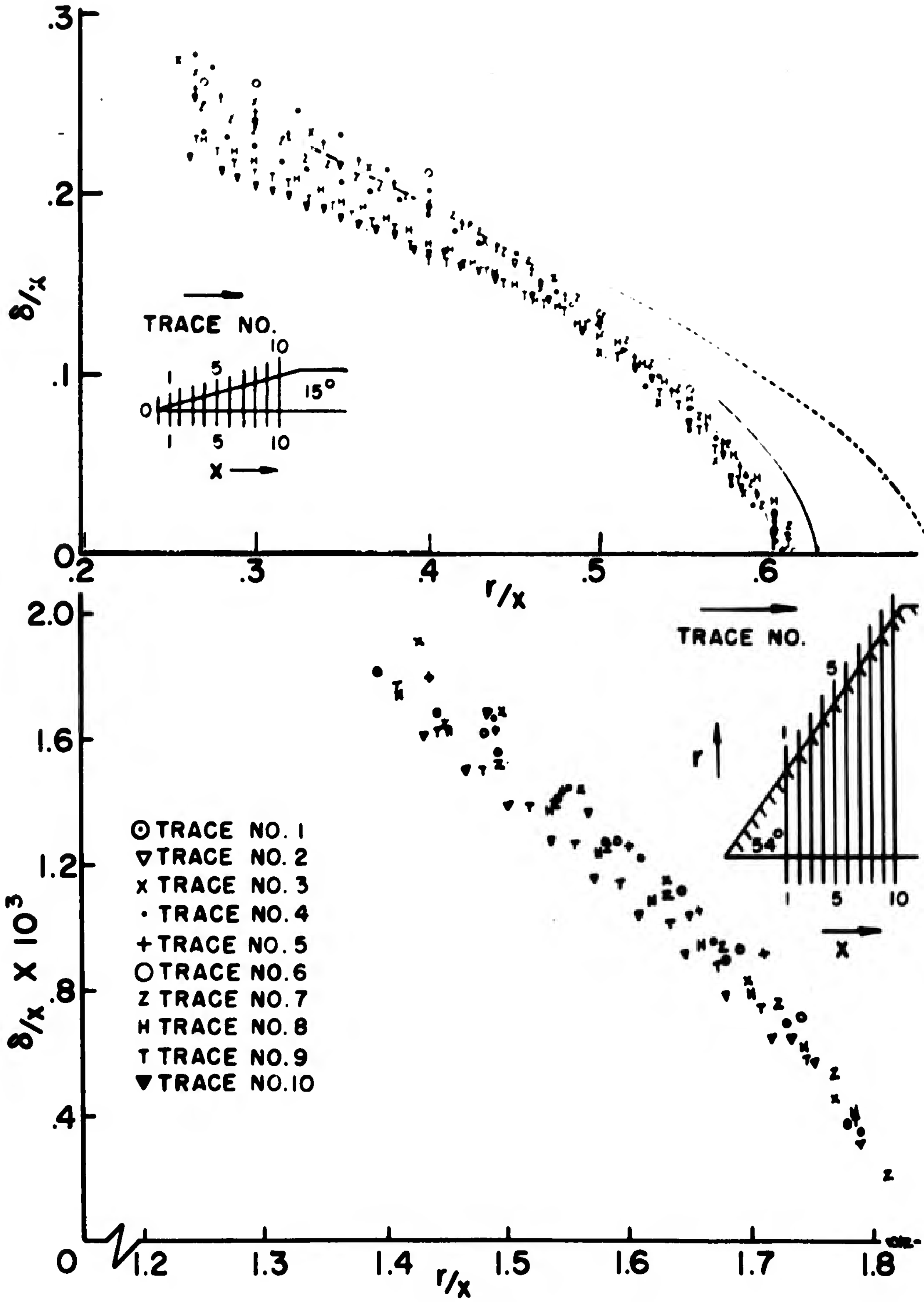

.3
.2
.1
0
δ/x
TRACE NO.
10
1
5
15°
0
1
5
10
X
.2
.3
.4
.5
.6
r/x
2.0
1.6
1.2
.8
.4
0
δ/x X 10³
TRACE NO. 1
TRACE NO. 2
X TRACE NO. 3
· TRACE NO. 4
+ TRACE NO. 5
TRACE NO. 6
Z TRACE NO. 7
H TRACE NO. 8
T TRACE NO. 9
TRACE NO. 10
TRACE NO.
5
1
r
54°
1
5
10
X
1.2
1.3
1.4
1.5
1.6
1.7
1.8
r/x

FIGURE 11

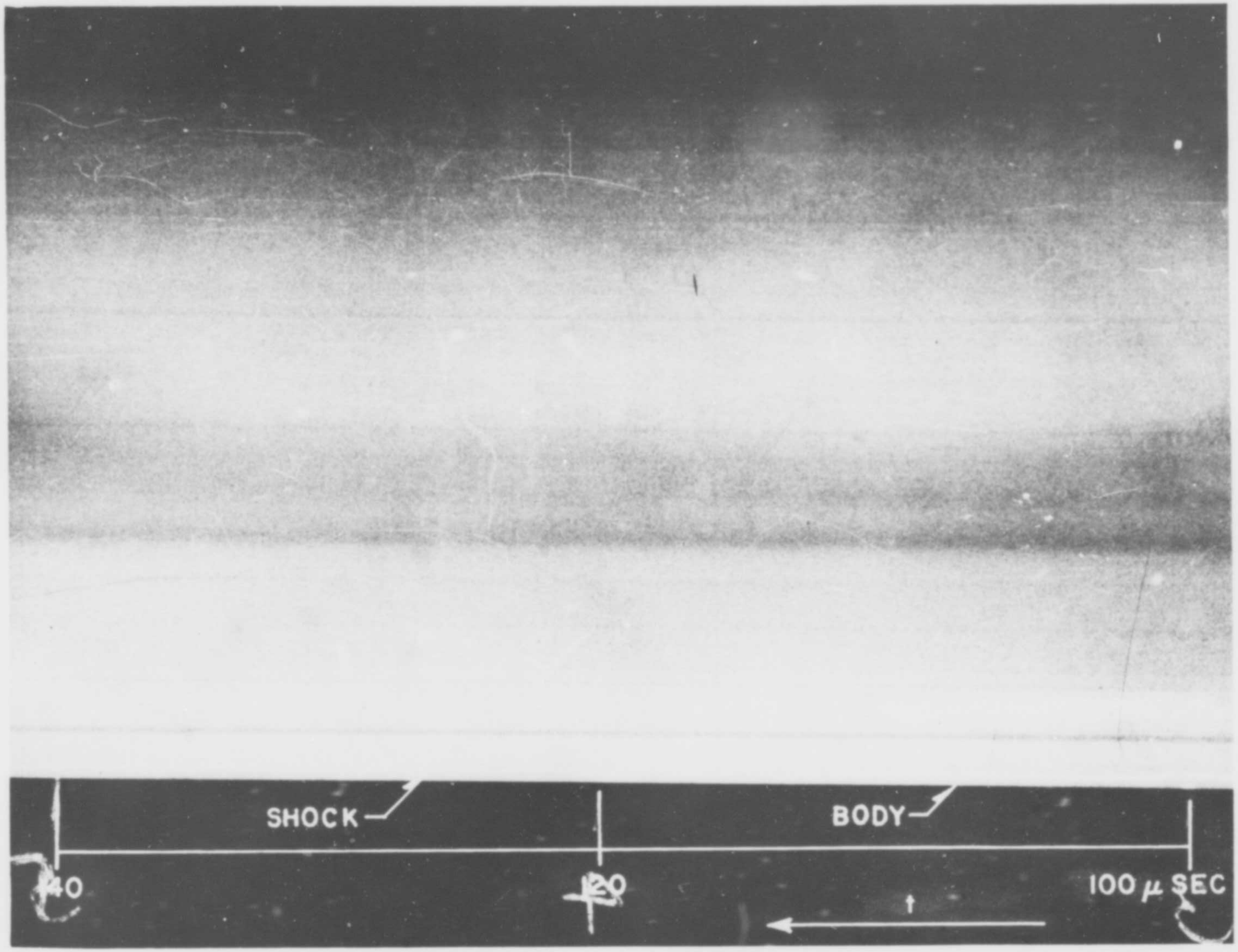

FIGURE 12

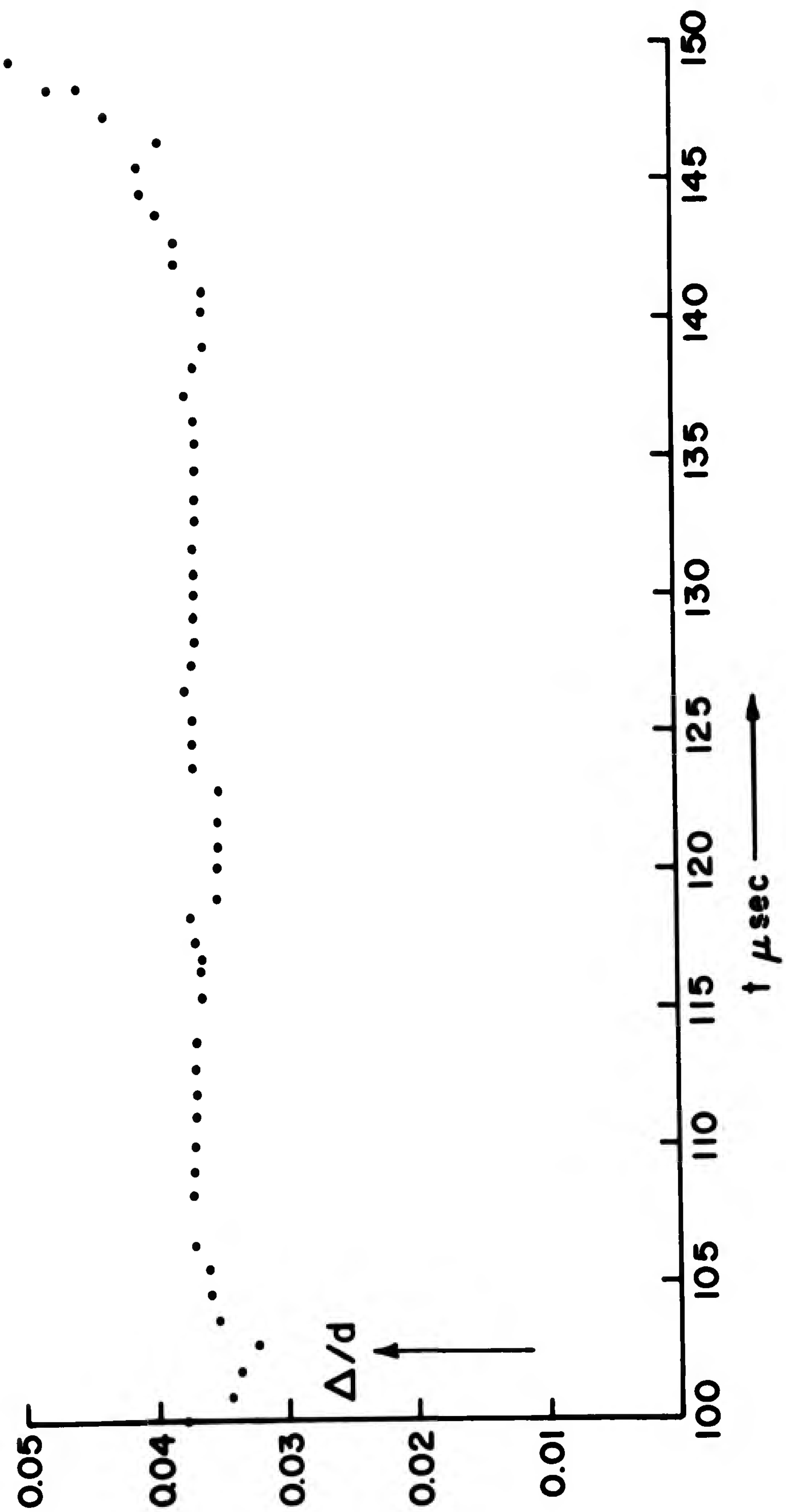
0.05
0.04
0.03
0.02
0.01
Δ/d
100
105
110
115
120
125
130
135
140
145
150
t μsec

FIGURE 13

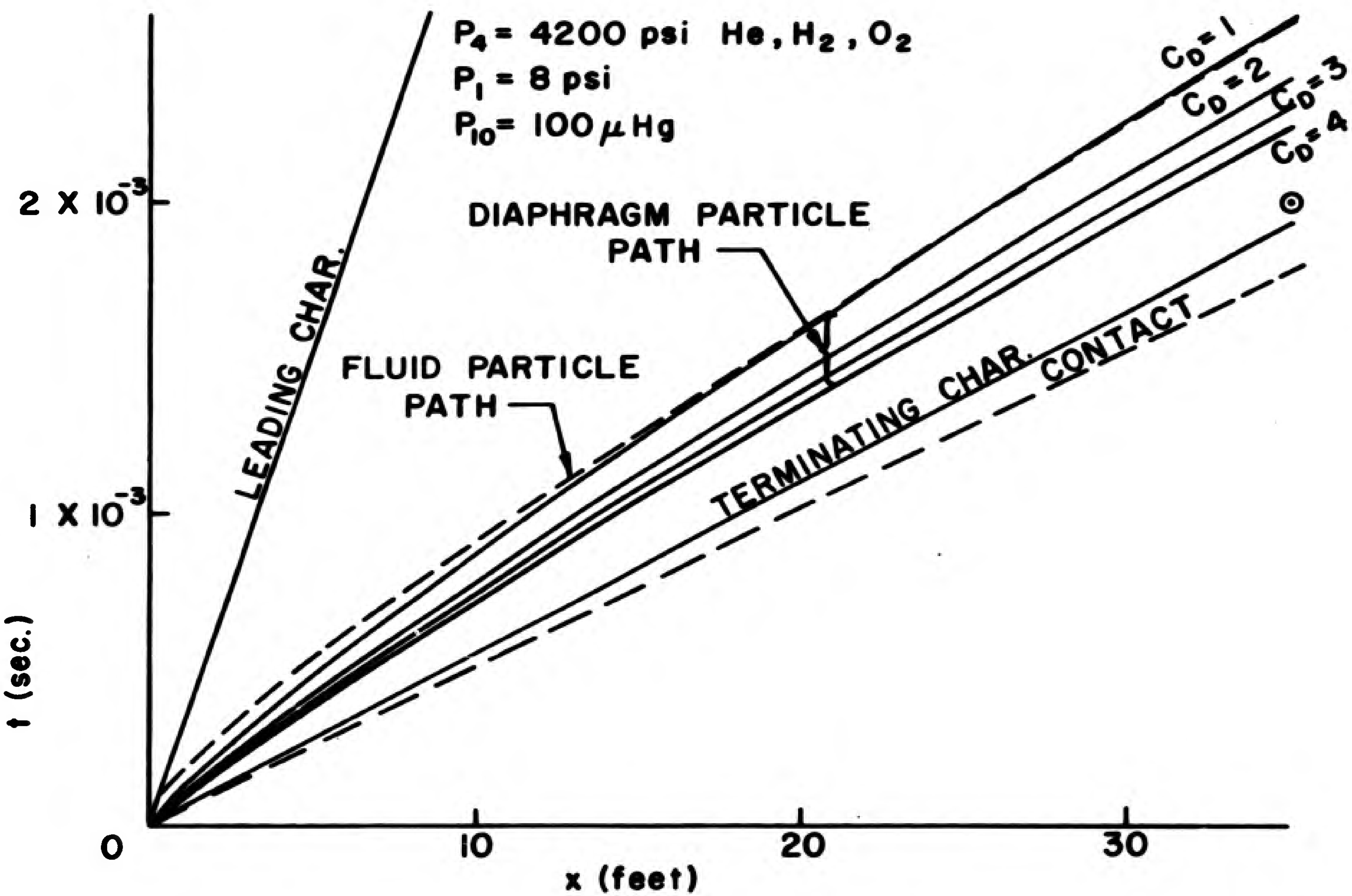

P4 = 4200 psi He, H2, O2
P1 = 8 psi
P10 = 100 μHg
LEADING CHAR.
DIAPHRAGM PARTICLE PATH
FLUID PARTICLE PATH
TERMINATING CHAR.
CONTACT
CD=1
CD=2
CD=3
CD=4
2 X 10^-3
1 X 10^-3
t (sec.)
0
10
20
30
x (feet)

FIGURE 14

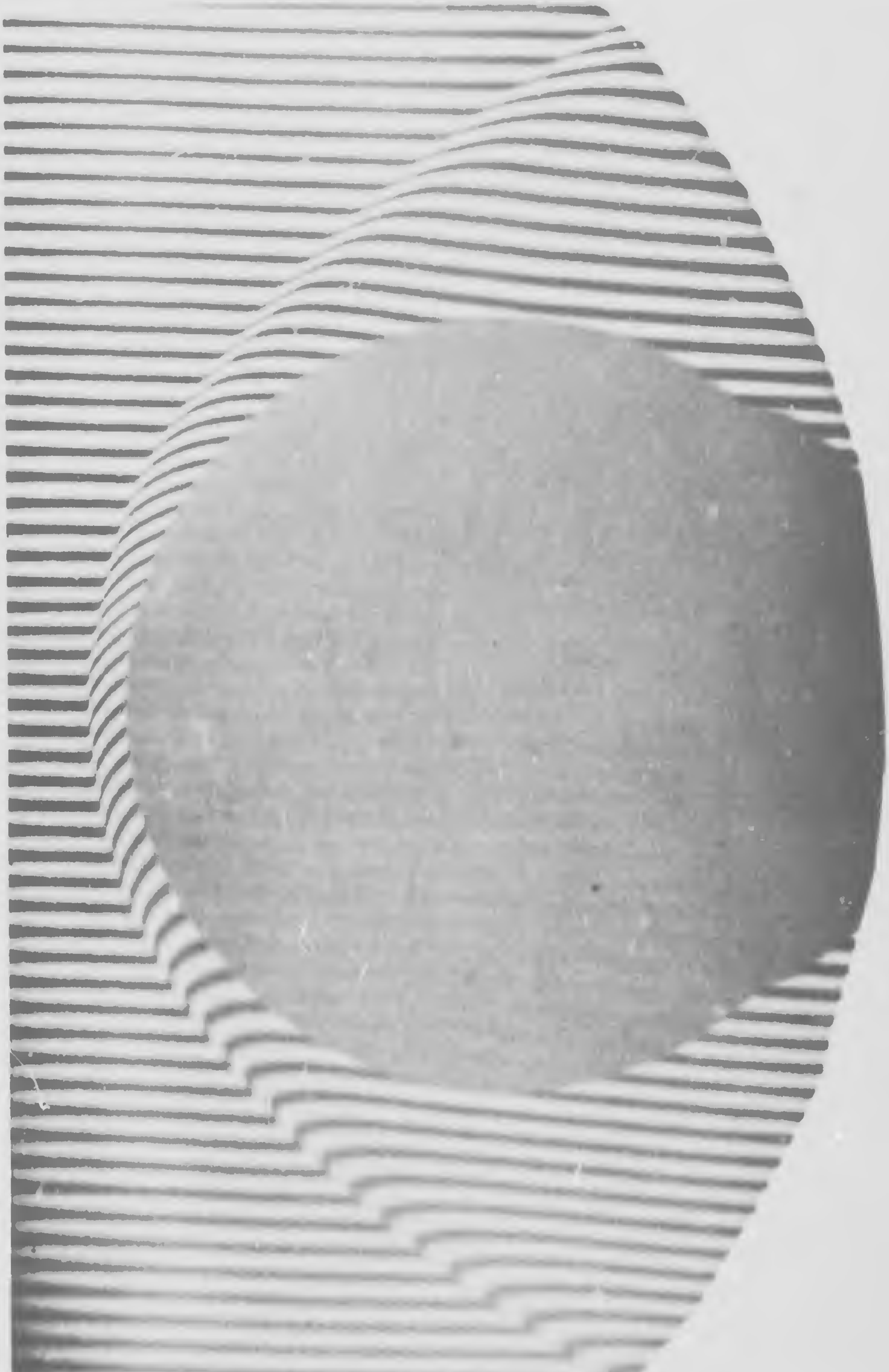

FIGURE 15

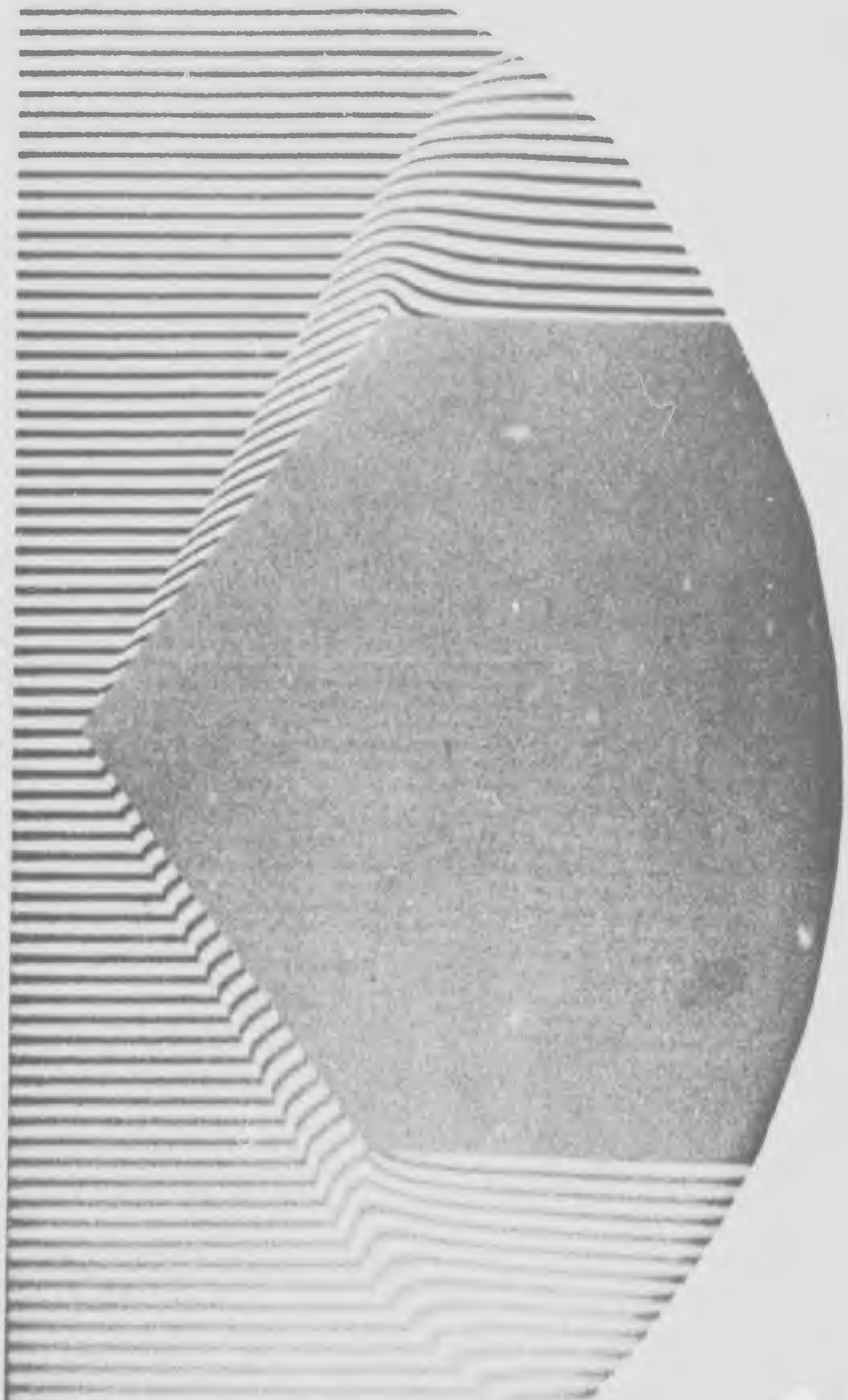

FIGURE 16

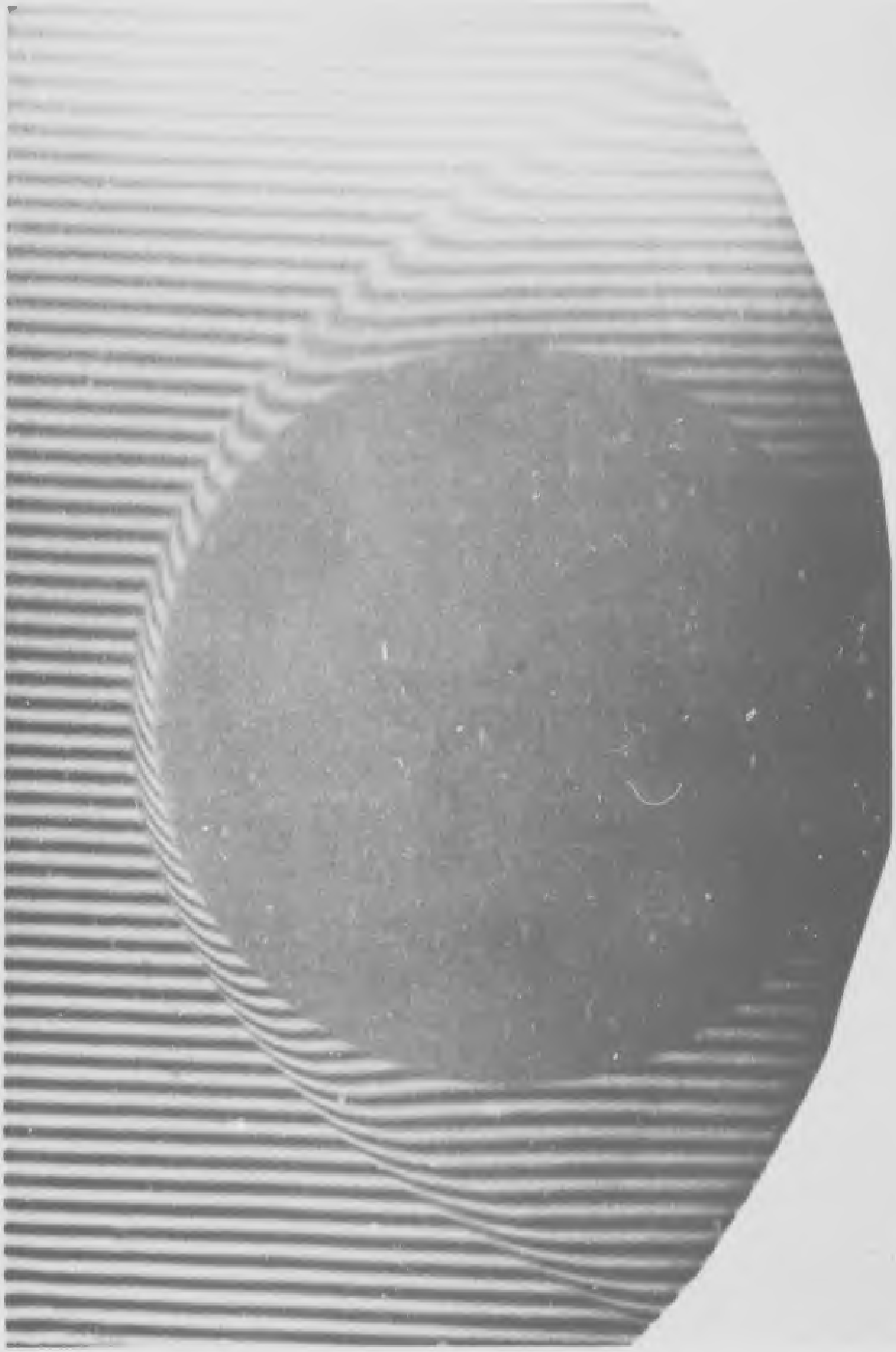

FIGURE 17

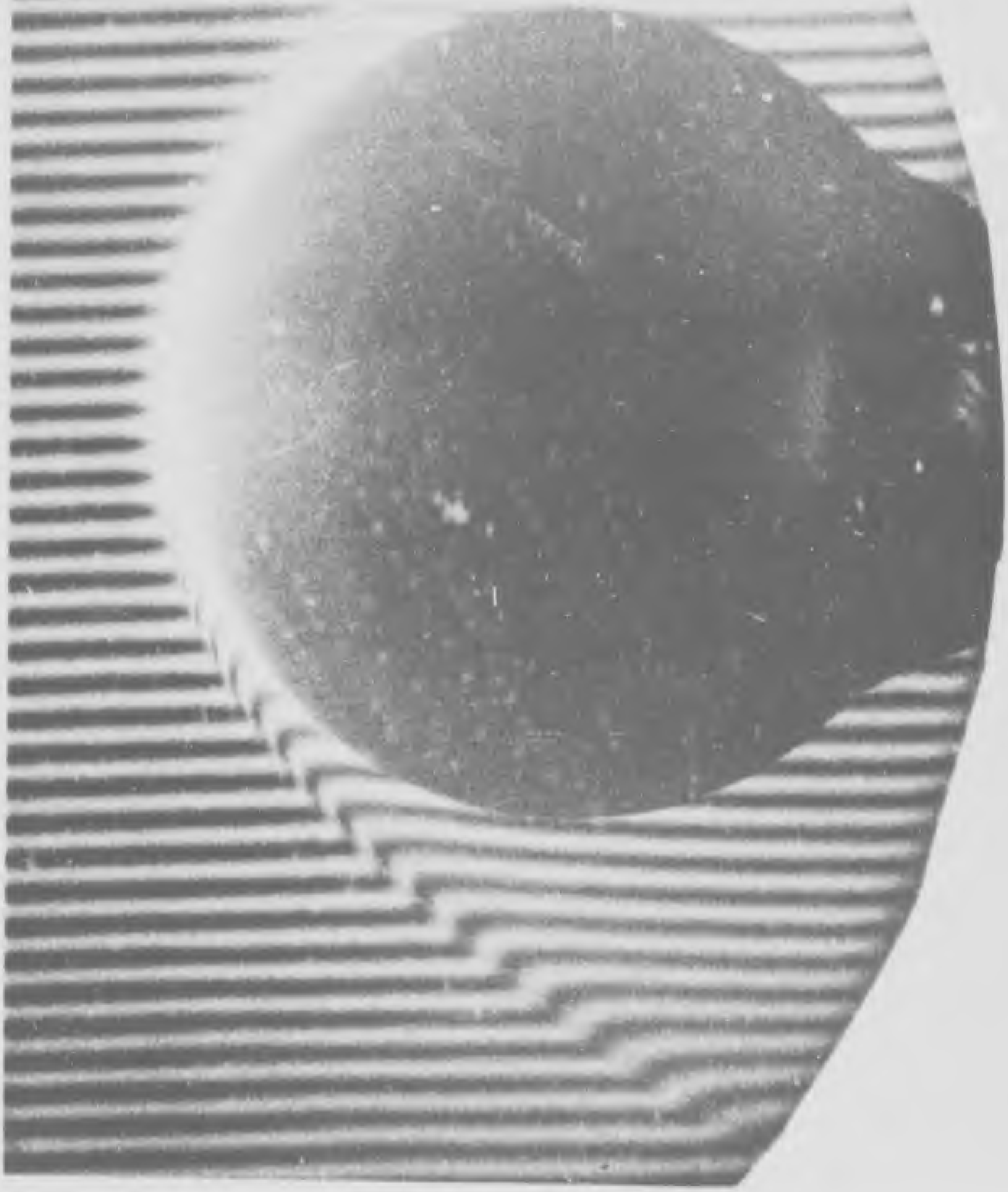

FIGURE 18

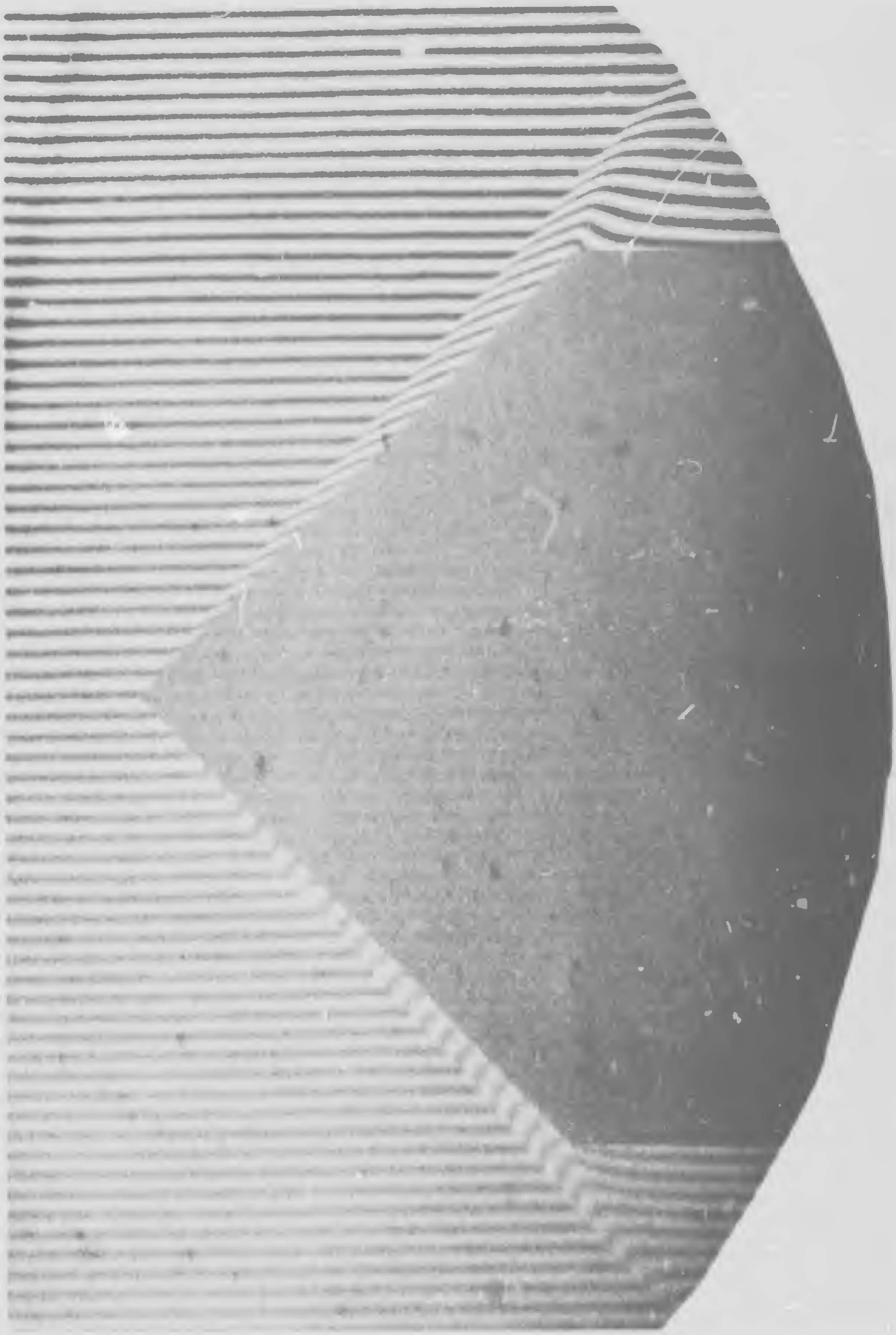

FIGURE 19

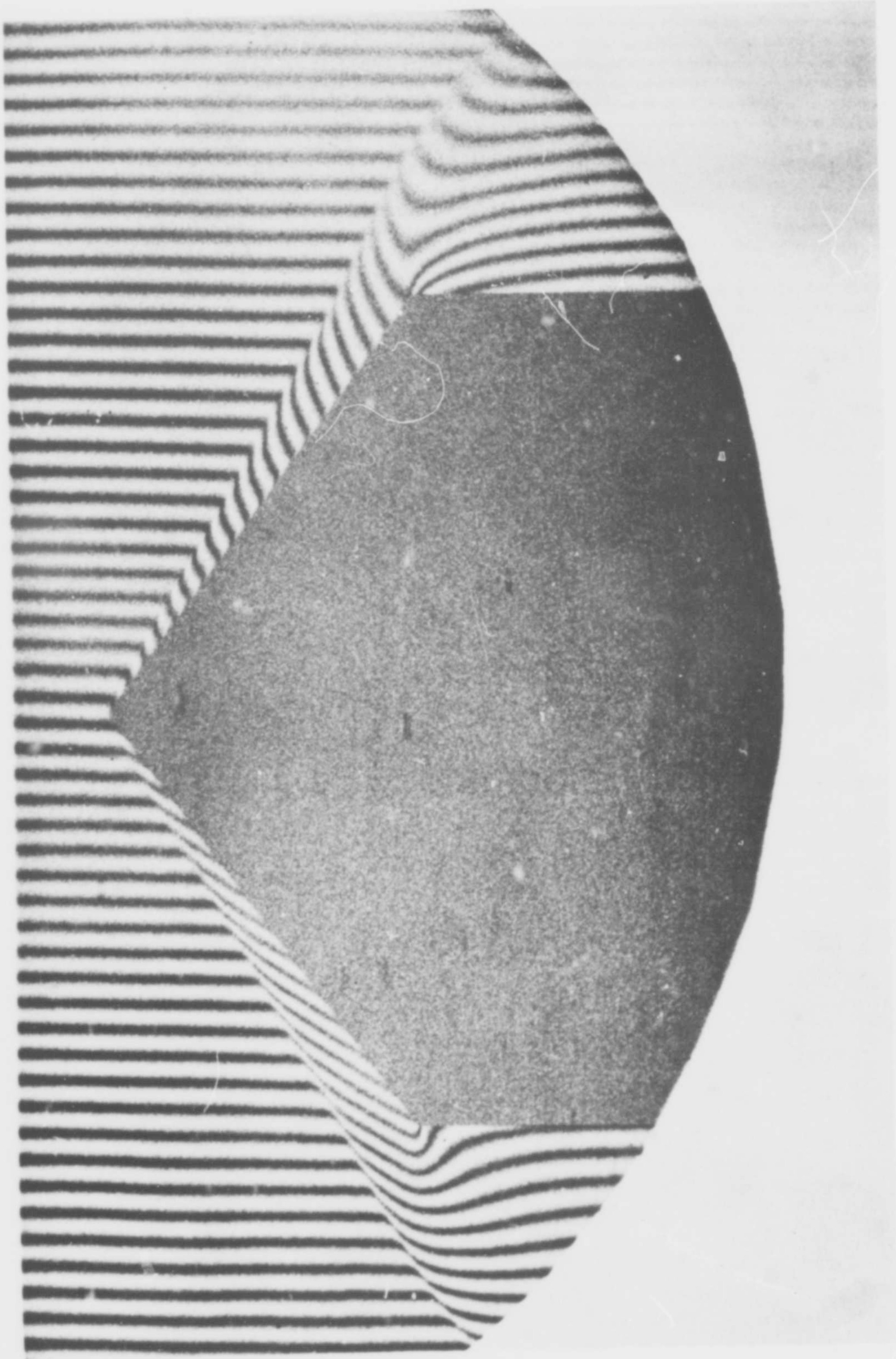

FIGURE 20

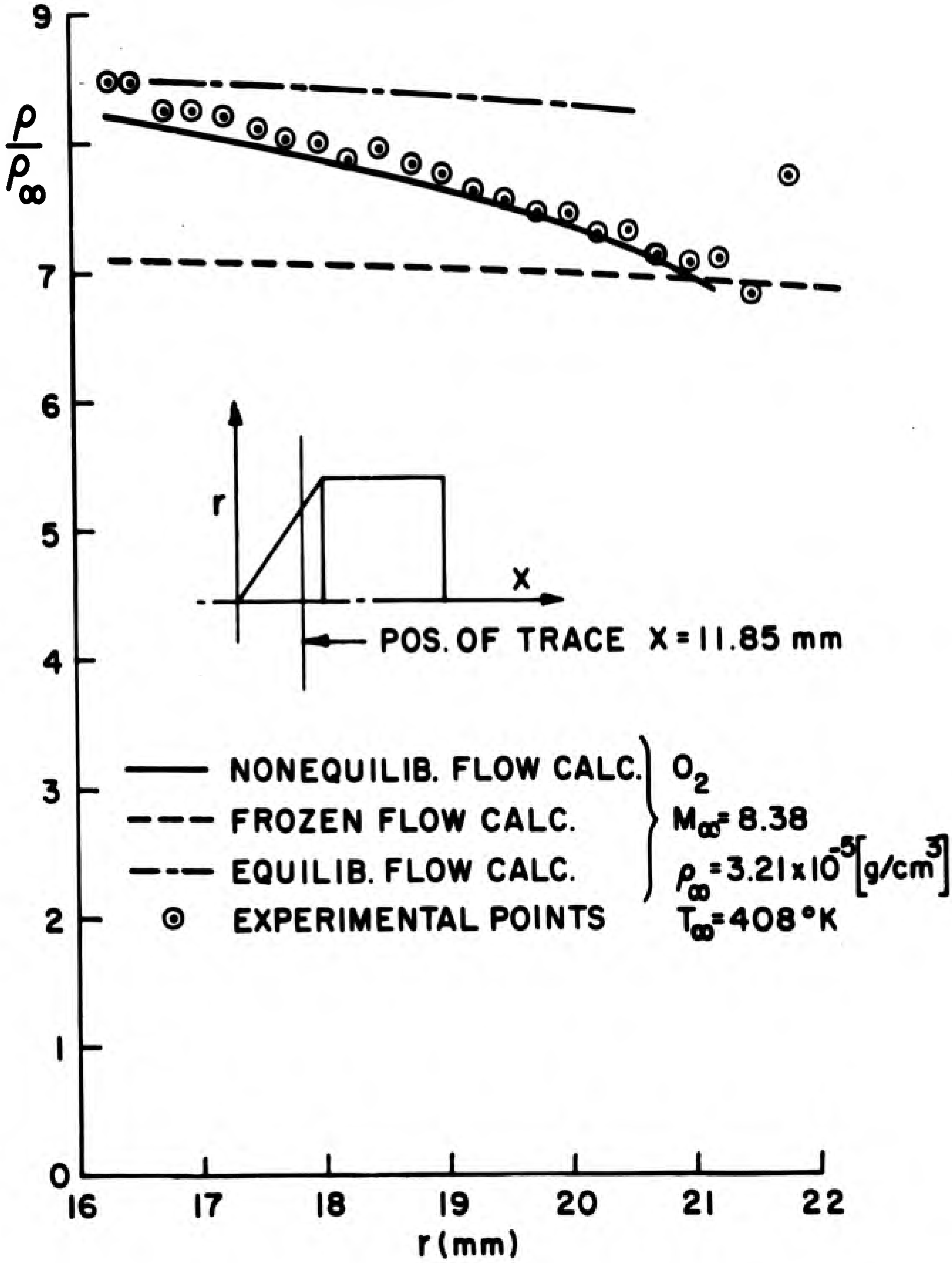
9
7
6
5
4
3
2
1
0
16
17
18
19
20
21
22
r (mm)
r
X
POS. OF TRACE X = 11.85 mm
NONEQUILIB. FLOW CALC.
FROZEN FLOW CALC.
EQUILIB. FLOW CALC.
EXPERIMENTAL POINTS
O_2
$M_\infty = 8.38$
$\rho_\infty = 3.21 \times 10^{-5} [g/cm^3]$
$T_\infty = 408\,°K$

FIGURE 21

REFERENCES

1. Hertzberg, A., Wittliff, C. H., and Hall, J. G. Cornell Aeron. Lab. No. AD-1052-A-12 (1961).

2. Trimpi, R. NASA TR R-133 (1962).

3. Spurk, J. H., and Shear, D. D. Ballistic Research Laboratories Report No. 1266 (1964).

4. Giese, J. H., Bennett, F. D., and Bergdolt, V. E. Journal of Applied Physics, 21, No. 12 (1950).

5. Whitfield, J. D., ARO, Inc. Private communication.

6. Roshko, A. Phys. of Fluids, 3, No. 6 (1960).

7. Spurk, J. H., Gerber, N., and Sedney, R. Ballistic Research Laboratories Report No. 1276 (1965). (To be published in AIAA Journal).

APPENDIX

The transistion piece consists of two parts which, upon assembly, produce the required transition from round to square (See Figure A1). Part I can be fabricated by first machining a surface of revolution in a tubular section as indicated in Figure A2. The tubular section is then faced off to fit inside a square, hollow pyramidal body (part II of Figure A1). After this process, part I consists of a tubular section with four prongs. These prongs serve as displacement bodies in the pyramidal body.

The generating curve of the surface of revolution is tabulated in Figure A3. It follows from elementary geometrical relations.

BLANK PAGE

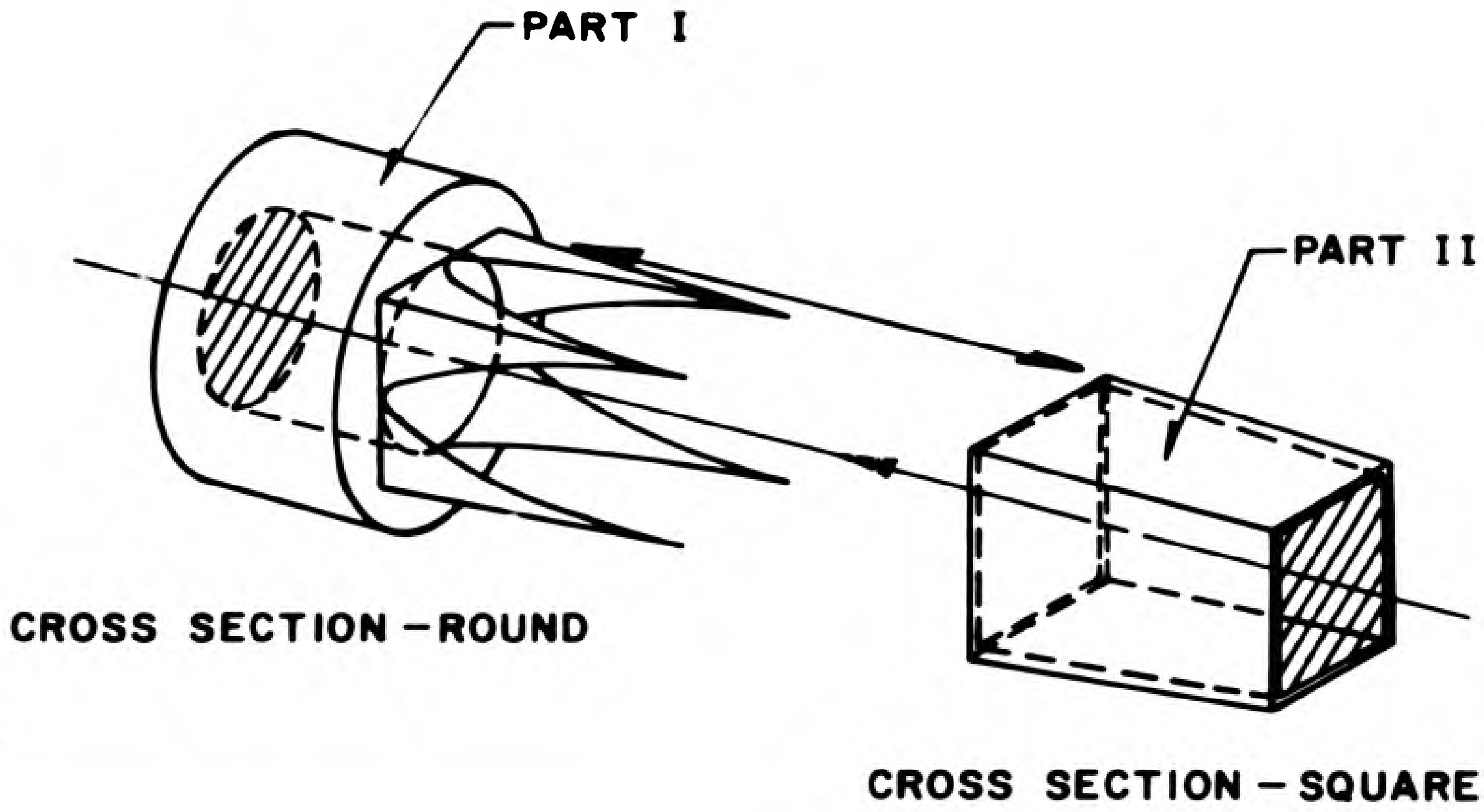

FIGURE 1A

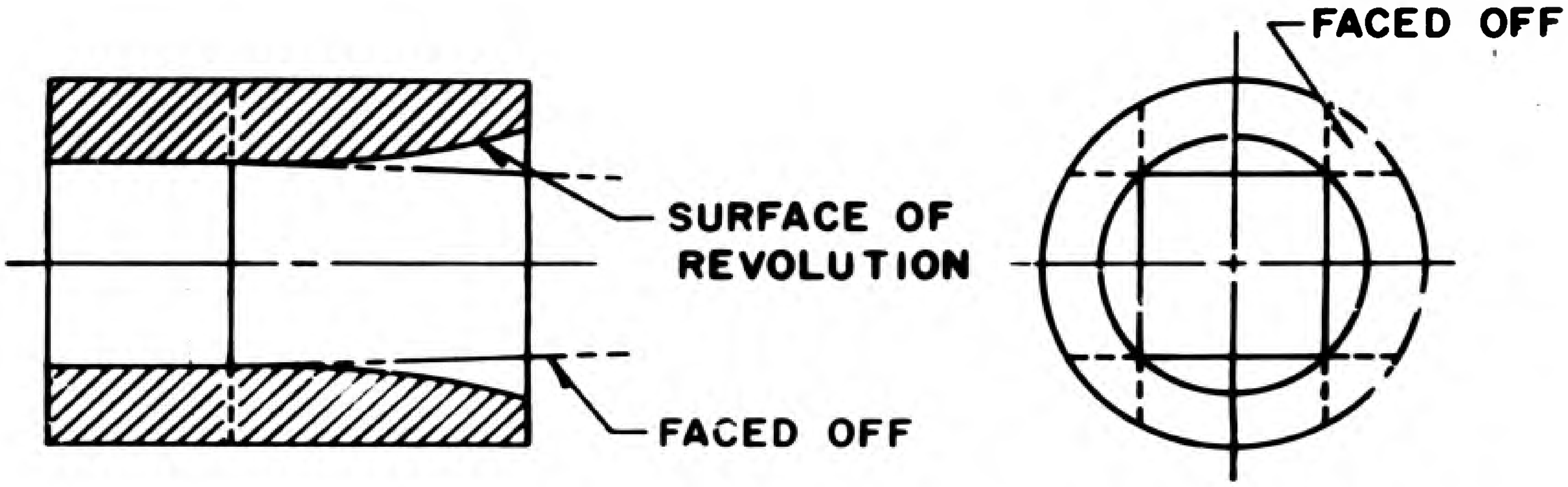

(TUBULAR SECTION)

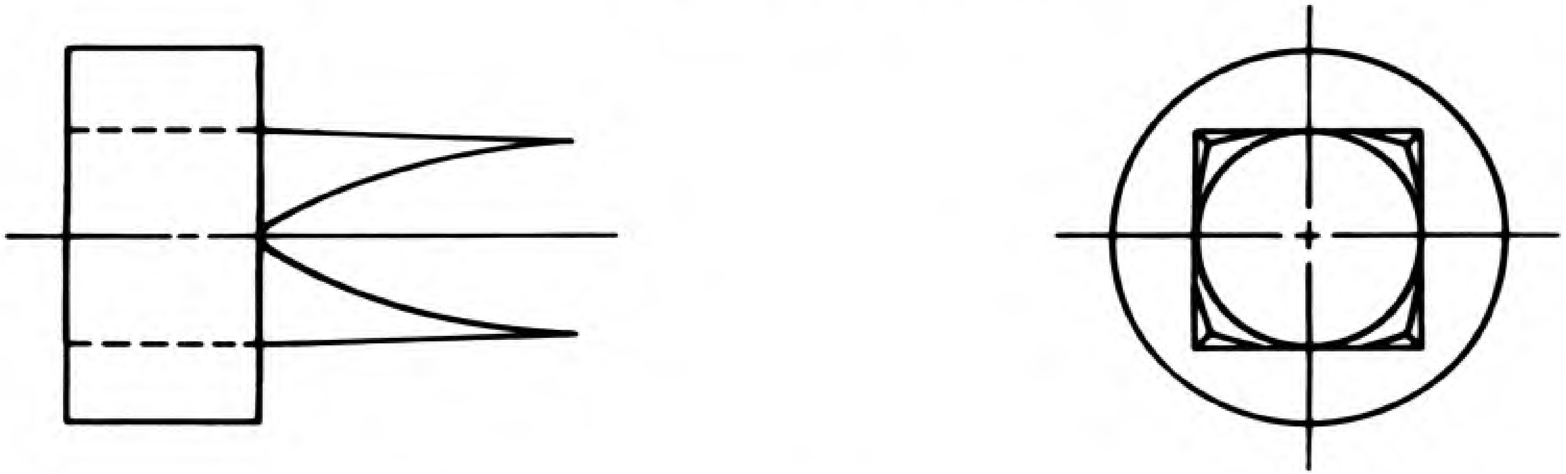

(TUBULAR SECTION AFTER FACING)

FIGURE 2A

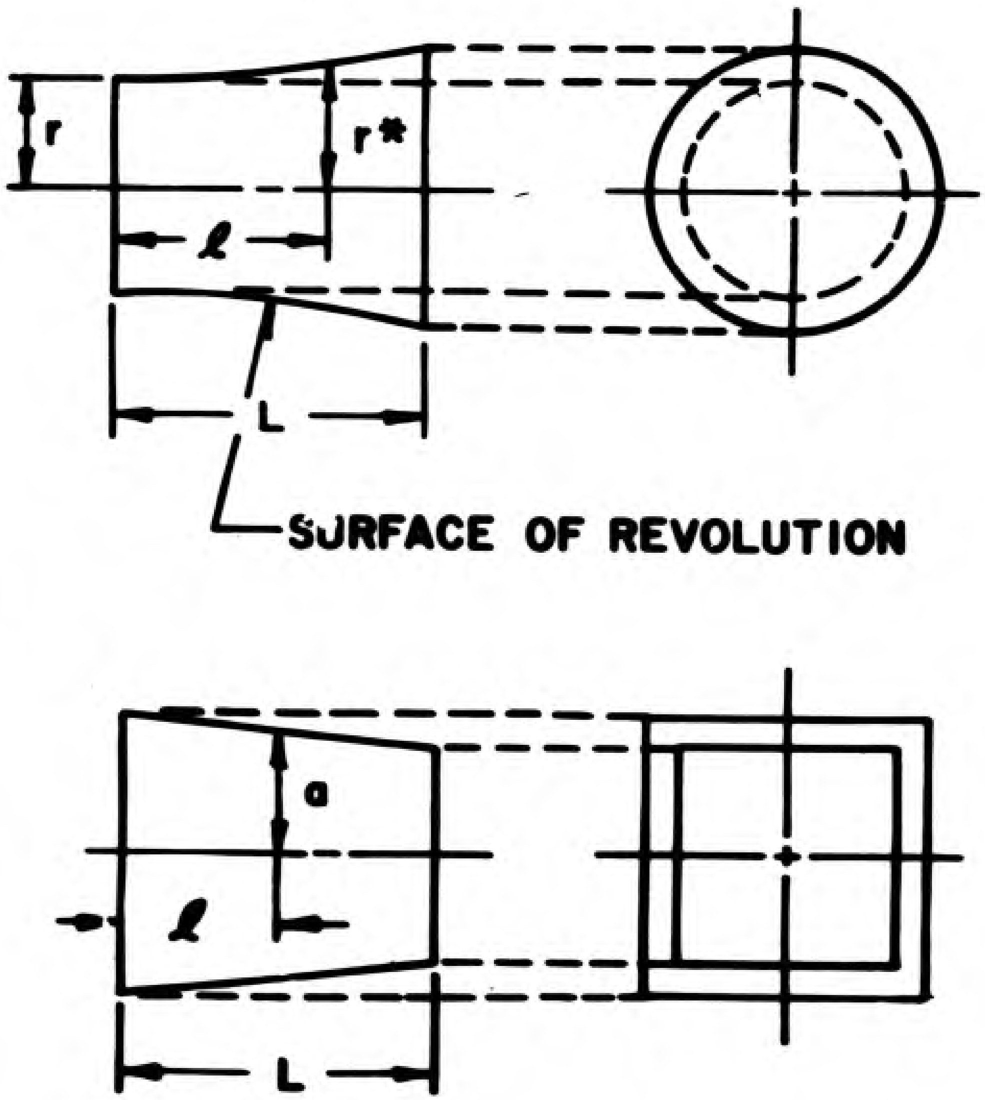

ℓ/L	$\frac{r^*}{r}$	a/r
0.	1.00000	1.0000
0.1	1.0018	
0.2	1.0058	
0.3	1.0117	
0.4	1.0199	
0.5	1.0308	Linear Dependence
0.6	1.0449	
0.7	1.0638	
0.8	1.0900	
0.9	1.1299	
1.0	1.2533	0.8862

FIGURE 3A

Unclassified
Security Classification

DOCUMENT CONTROL DATA - R&D

(Security classification of title, body of abstract and indexing annotation must be entered when the overall report is classified)

1. ORIGINATING ACTIVITY (Corporate author) U.S. Army Ballistic Research Laboratories Aberdeen Proving Ground, Md.	2a. REPORT SECURITY CLASSIFICATION Unclassified 2b. GROUP

3. REPORT TITLE

DESIGN, OPERATION AND PRELIMINARY RESULTS OF THE BRL EXPANSION TUBE

4. DESCRIPTIVE NOTES (Type of report and inclusive dates)

5. AUTHOR(S) (Last name, first name, initial)

Spurk, Joseph H.

6. REPORT DATE	7a. TOTAL NO. OF PAGES	7b. NO. OF REFS
October 1965	51	7

8a. CONTRACT OR GRANT NO.	9a. ORIGINATOR'S REPORT NUMBER(S) Report No. 1304
b. PROJECT NO. 1P222901A201 c. d.	9b. OTHER REPORT NO(S) (Any other numbers that may be assigned this report)

10. AVAILABILITY/LIMITATION NOTICES

Distribution of this report in unlimited.

11. SUPPLEMENTARY NOTES	12. SPONSORING MILITARY ACTIVITY U.S. Army Materiel Command Washington, D. C.

13. ABSTRACT

Thispaper describes the Ballistic Research Laboratories expansion tube, which has been built for interferometric observation of hypersonic flow fields. The optical instrumentation consists of a Mach-Zehnder interferometer in conjunction with a rotating mirror and frame camera. By means of simultaneous streak interferometry the free stream conditions are monitored and determined for each test run. With the free stream condition known, the frame interferogram of the flow around the model can be evaluated to give density or electron density field around the model. Examples of density distribution in the free stream are shown for two typical cases, with flow velocity of ~ 10,000 and 20,000 ft/sec, respectively. The density distribution within the shock layer of a reacting flow is shown and compared with theoretical prediction. Conical flow tests are performed in an attempt to assess the free stream turbulence. The effects of second diaphragm and the flow contamination are discussed.

DD FORM 1 JAN 64 1473

Unclassified
Security Classification

Unclassified
Security Classification

14. KEY WORDS	LINK A		LINK B		LINK C	
	ROLE	WT	ROLE	WT	ROLE	WT
Experimental Hypersonic flow High enthalpy flow Nonequilibrium flow Interferometer						

INSTRUCTIONS

1. ORIGINATING ACTIVITY: Enter the name and address of the contractor, subcontractor, grantee, Department of Defense activity or other organization *(corporate author)* issuing the report.

2*a*. REPORT SECURITY CLASSIFICATION: Enter the overall security classification of the report. Indicate whether "Restricted Data" is included. Marking is to be in accordance with appropriate security regulations.

2*b*. GROUP: Automatic downgrading is specified in DoD Directive 5200.10 and Armed Forces Industrial Manual. Enter the group number. Also, when applicable, show that optional markings have been used for Group 3 and Group 4 as authorized.

3. REPORT TITLE: Enter the complete report title in all capital letters. Titles in all cases should be unclassified. If a meaningful title cannot be selected without classification, show title classification in all capitals in parenthesis immediately following the title.

4. DESCRIPTIVE NOTES: If appropriate, enter the type of report, e.g., interim, progress, summary, annual, or final. Give the inclusive dates when a specific reporting period is covered.

5. AUTHOR(S): Enter the name(s) of author(s) as shown on or in the report. Enter last name, first name, middle initial. If military, show rank and branch of service. The name of the principal author is an absolute minimum requirement.

6. REPORT DATE: Enter the date of the report as day, month, year; or month, year. If more than one date appears on the report, use date of publication.

7*a*. TOTAL NUMBER OF PAGES: The total page count should follow normal pagination procedures, i.e., enter the number of pages containing information.

7*b*. NUMBER OF REFERENCES: Enter the total number of references cited in the report.

8*a*. CONTRACT OR GRANT NUMBER: If appropriate, enter the applicable number of the contract or grant under which the report was written.

8*b*, 8*c*, & 8*d*. PROJECT NUMBER: Enter the appropriate military department identification, such as project number, subproject number, system numbers, task number, etc.

9*a*. ORIGINATOR'S REPORT NUMBER(S): Enter the official report number by which the document will be identified and controlled by the originating activity. This number must be unique to this report.

9*b*. OTHER REPORT NUMBER(S): If the report has been assigned any other report numbers *(either by the originator or by the sponsor)*, also enter this number(s).

10. AVAILABILITY/LIMITATION NOTICES: Enter any limitations on further dissemination of the report, other than those imposed by security classification, using standard statements such as:

(1) "Qualified requesters may obtain copies of this report from DDC."

(2) "Foreign announcement and dissemination of this report by DDC is not authorized."

(3) "U. S. Government agencies may obtain copies of this report directly from DDC. Other qualified DDC users shall request through
_______________."

(4) "U. S. military agencies may obtain copies of this report directly from DDC. Other qualified users shall request through
_______________."

(5) "All distribution of this report is controlled. Qualified DDC users shall request through
_______________."

If the report has been furnished to the Office of Technical Services, Department of Commerce, for sale to the public, indicate this fact and enter the price, if known.

11. SUPPLEMENTARY NOTES: Use for additional explanatory notes.

12. SPONSORING MILITARY ACTIVITY: Enter the name of the departmental project office or laboratory sponsoring *(paying for)* the research and development. Include address.

13. ABSTRACT: Enter an abstract giving a brief and factual summary of the document indicative of the report, even though it may also appear elsewhere in the body of the technical report. If additional space is required, a continuation sheet shall be attached.

It is highly desirable that the abstract of classified reports be unclassified. Each paragraph of the abstract shall end with an indication of the military security classification of the information in the paragraph, represented as *(TS)*, *(S)*, *(C)*, *or (U)*.

There is no limitation on the length of the abstract. However, the suggested length is from 150 to 225 words.

14. KEY WORDS: Key words are technically meaningful terms or short phrases that characterize a report and may be used as index entries for cataloging the report. Key words must be selected so that no security classification is required. Identifiers, such as equipment model designation, trade name, military project code name, geographic location, may be used as key words but will be followed by an indication of technical context. The assignment of links, rules, and weights is optional.

Unclassified
Security Classification